Andean Geology 53 (2): 176-205. May, 2026
doi: 10.5027/andgeoV53n2-3876

Andean Geology
www.andeangeology.cl

SPECIAL ISSUE: RESEARCH ON THE SOUTH WEST MARGIN OF GONDWANA

Stratigraphic and structural reappraisal of the metamorphic complex of NE Cordillera Darwin, Tierra del Fuego, Chile

***Pablo J. Torres Carbonell[1], Sebastián J. Cao[2], Fernando A. Poblete[3], Marc Poujol[4]**

[1] *Centro Austral de Investigaciones Científicas (CADIC), Bernardo Houssay 200, Ushuaia, Argentina.*
Present address: INGEOSUR (CONICET), Alem 1253 cuerpo B' 1° Piso, Bahía Blanca, Argentina.
Orcid ID: https://orcid.org/0000-0003-2804-8789
poltorrescarbonell@gmail.com

[2] *Instituto de Ciencias Polares, Ambiente y Recursos Naturales, Universidad de Tierra del Fuego, Fuegia Basket 251 3° Piso, Ushuaia, Argentina.*
Orcid ID: https://orcid.org/0000-0003-2307-3993
sebacao@gmail.com

[3] *Departamento de Geología, Facultad de Ciencias Físicas y Matemáticas, Universidad de Chile, Plaza Ercilla 803, Santiago, Chile.*
Orcid ID: https://orcid.org/0000-0002-2140-5483
ferpoble@uchile.cl

[4] *Univ. Rennes, CNRS, Géosciences Rennes, UMR6118, F-35000 Rennes, France.*
Orcid ID: https://orcid.org/0000-0001-8682-2926
marc.poujol@univ-rennes.fr

* *Corresponding author. poltorrescarbonell@gmail.com*

ABSTRACT. New petrographic and structural studies in NE Cordillera Darwin have impacts on the stratigraphic distinction between basement and cover of the Rocas Verdes Basin. Our results reveal that metasedimentary and metavolcanic rocks mapped in the hanging wall and footwall of the first-order Glaciar Marinelli Thrust were affected by the same episodes of Meso-Cenozoic deformation as the cover rocks of the Fuegian Andes, with no evidence of pre-Jurassic deformation. The key to determining the deformation sequence relies on correct interpretation of the primary sedimentary layering in fine-grained metasedimentary rocks. Our results suggest that the rocks in the study area are part of the sedimentary and volcanic fill of the Rocas Verdes Basin. Two new U-Pb age determinations indicate that early Paleozoic and older detrital zircon grains prevail in these cover rocks, consistent with provenance from an eroded Paleozoic basement during the early development of the rift basin. Careful petrographic studies are required to assess the validity of detrital zircon maximum depositional ages in the area.

Keywords: Structural geology, Stratigraphy, Metasedimentary cover, Rocas Verdes Basin, Fuegian Andes, Cordillera Darwin.

RESUMEN. Reevaluación estratigráfica y estructural del complejo metamórfico del noreste de la Cordillera Darwin, Tierra del Fuego, Chile. Nuevos estudios petrográficos y estructurales en el noreste de la Cordillera Darwin nos permiten distinguir estratigráficamente entre el basamento y la cobertura de la Cuenca Rocas Verdes. Estos resultados muestran que las rocas metasedimentarias y metavolcánicas mapeadas en los bloques yacente y colgante del corrimiento Glaciar Marinelli fueron afectadas por los mismos episodios de deformación meso-cenozoica que las rocas en la cobertura de los Andes Fueguinos, sin evidencias de deformación prejurásica. La clave para definir la secuencia de deformación está en la correcta distinción de la laminación primaria en las rocas metasedimentarias de grano fino. Los resultados sugieren que las rocas estudiadas son parte del relleno sedimentario y volcánico de la Cuenca Rocas Verdes. Dos nuevas dataciones por U-Pb indican que en estas rocas predominan circones detríticos del Paleozoico temprano o más antiguos, lo cual es consistente con la proveniencia desde un basamento paleozoico erosionado durante el desarrollo temprano del *rift*. La validez de las edades máximas de sedimentación a partir de dataciones en circones detríticos en el área debe ser evaluada mediante estudios petrográficos de detalle.

Palabras clave: Geología estructural, Estratigrafía, Cobertura metasedimentaria, Cuenca Rocas Verdes, Andes Fueguinos, Cordillera Darwin.

1. Introduction

Stratigraphic interpretation of metasedimentary facies in the Fuegian Andes is a problematic issue that geologists have had to confront since the earliest geological studies in this region. In some areas the degree of deformation is such that separation between stratigraphic units based exclusively on lithology is not possible. In recent years, geochronological determinations allowed distinction between units with very similar lithologies (*e.g.*, phyllites or slates). Although helping to separate Cretaceous and Jurassic units with synsedimentary tuffaceous components, this approach has limitations when dealing with sedimentary facies that were not contemporary with volcanism.

Determining the stratigraphic order of mostly fine-grained metasedimentary rocks of the Paleozoic basement and Mesozoic sedimentary cover in the Fuegian Andes is especially challenging. The facies similarity between some horizons in these rock units has been recognized since the early investigations in Cordillera Darwin (Kranck, 1932; Fester, 1938). Strong deformation and regional metamorphism during the Late Cretaceous largely obliterated original stratigraphic relationships, hampering distinction in the field (Kranck, 1932; Johnson, 1990; Hervé *et al.*, 2010a). In addition, the scarcity of zircon coeval with sedimentation in the protoliths usually rules out geochronological distinction, a problem that extends beyond the local area of the Fuegian Andes (Hervé *et al.*, 2010a; Cawood *et al.*, 2012; Rossignol *et al.*, 2019; Copeland, 2020; Cao *et al.*, 2022; Castillo *et al.*, 2022).

Here we report a detailed revision of the rocks exposed in NE Cordillera Darwin, a region with contrasting stratigraphic interpretations of the basement and cover units. We consider that detailed petrographic analysis, together with the identification of structural generations from macroscopic and microstructural studies, is key to separating basement from cover. Mineral dating (*e.g.*, detrital zircon U-Pb ages), however, may be of limited value when the objective is to determine the true stratigraphic position of these rocks, which rarely had coeval volcanism. Our updated review, based on new mapping, petrographic and microstructural analyses, allows us to improve the geological map accuracy of this area and organize the stratigraphic and structural framework, with the aims of unifying criteria and facilitating future research in such a complex terrane.

2. Geological setting

2.1. Deformation events and metamorphism in the central belt of the Fuegian Andes

Cordillera Darwin is the structural culmination of the Fuegian Andes. It exposes Paleozoic basement of the southwestern margin of Gondwana and overlying Mesozoic cover rocks exhibiting intense Cretaceous and Cenozoic deformation. The cover rocks were deposited in a Jurassic volcano-tectonic rift basin that evolved into a back-arc basin (Rocas Verdes Basin), with active marine sedimentation lasting until the end of the Early Cretaceous (Katz, 1963; Dalziel *et al.*, 1974; Suárez and Pettigrew, 1976; Wilson, 1991; Olivero and Martinioni, 2001). These rocks, whose stratigraphic framework is described below, were affected by two main episodes of deformation, associated with the Late Cretaceous closure of the basin and the Cenozoic formation of a retro-arc thrust-fold belt, respectively. Closure of the Rocas Verdes Basin involved north-northeastward obduction of the basin floor and south-southwestward underthrusting of its continental margin, followed by collision of this margin with the subduction-related magmatic arc (Nelson *et al.*, 1980; Dalziel, 1986; Cunningham, 1995; Klepeis *et al.*, 2010). The evolution of the thrust-fold belt included the development of duplex thrust systems and transference of shortening towards the retro-arc foreland basin, leading to exhumation of the internal orogen in the central belt (Álvarez-Marrón *et al.*, 1993; Rojas and Mpodozis, 2006; Klepeis *et al.*, 2010; Torres Carbonell *et al.*, 2020; Cao *et al.*, 2023).

The central belt of the Fuegian Andes (Fig. 1) thus involves rocks deformed by two main events. These are briefly introduced here, while a more detailed description of structures pertaining to our study area is given in section 2.3. The first generation of structures, caused by the closure of the Rocas Verdes Basin, involved intense deformation associated with the development of ductile shear zones and thrusts during obduction and underthrusting (Fig. 1). This deformation was coeval with regional metamorphism, with the higher grades (upper amphibolite facies) attained by the basin fill and its basement at mid-crustal levels between 90 and 70 Ma (Cunningham, 1994, 1995; Kohn *et al.*, 1995; Klepeis *et al.*, 2010; Maloney *et al.*, 2011). The lower metamorphic grades are shown by phyllites and slates of the uppermost

structural levels, comprising the metamorphosed Cretaceous sedimentary cover of the Rocas Verdes Basin and the foreland basin initiated during this orogenesis. These rocks suffered varying intensities of ductile deformation (Bruhn, 1979; Nelson *et al.*, 1980; Torres Carbonell *et al.*, 2017), which in the central belt was labelled $D1_{CB}$ by Torres Carbonell *et al.* (2020; CB: central belt, Fig. 1).

The second generation of structures recognized in the central belt includes mostly brittle-ductile and brittle faults, which comprise the roots of the Fuegian thrust-fold belt (Klepeis, 1994; Rojas and Mpodozis, 2006; Torres Carbonell *et al.*, 2020; Cao *et al.*, 2023). These thrust faults are interpreted as responsible for exhumation of the mid-crustal rocks exposed in the central belt, *i.e.*, the higher-grade metamorphic rocks juxtaposed with the shallower cover rocks of the Rocas Verdes Basin. In the more deformed rocks, the thrusts formed simultaneously with some ductile deformation, such as development of a crenulation cleavage, often localized near the fault zones and sparser or absent towards the foreland (Cao *et al.*, 2023). Thrust stacking in the central belt enables the study of different structural levels of the earlier $D1_{CB}$ deformation. The development of the thrust-fold belt and related structures was labelled $D2_{CB}$ (Torres Carbonell *et al.*, 2020; Fig. 1).

2.2. Central belt stratigraphy

2.2.1. Historical perspective

The currently accepted stratigraphic framework of Cordillera Darwin is the result of almost 100 years of geological investigation. In table 1 we provide a synthesis of the stratigraphic nomenclature of the main units addressed here and its modifications in successive studies, which helps to correlate stratigraphic names through time. We restrict our analysis to the northern flank of Cordillera Darwin, where low-grade metamorphic rocks crop out. The higher-grade rocks, cropping out in fjords on the southern flank, include a complex tectonized mixture of several units (cf. Klepeis *et al*., 2010), whose analysis is beyond the objective of this work.

The first detailed petrological study of Cordillera Darwin was published by E. Kranck in 1932. His initial rough stratigraphic separation distinguished: 1) "*high metamorphic, micaceous and quartzitic schists of the Darwin Cordillera and its westerly and easterly continuation*", and 2) "*argillitic and phtanitic schists of the Beagle regions and north front of the Central Cordillera (Mount Buckland and Yahgan Formations)*" (pp. 25-26). The first unit is distributed in what the author called the "central core of the High Cordillera", which occupies the area between Ushuaia and Península Brunswick (Fig. 1), and consists of "*strongly tectonized and recrystallized schists*" and abundant "*altered greenstones*", metamorphosed into chlorite- and talc-schists. The second unit (Monte Buckland and Yahgan formations) is now included in the Tobífera Formation-Lemaire Complex and the Yahgan Formation, which are described in the next section.

Although Kranck (1932) is frequently cited for recognizing the "unconformity" between the metamorphic basement of Cordillera Darwin and its cover, this surface is not actually exposed and was interpreted on the basis of the stratigraphic relationships exposed in northern Fiordo De Agostini (Monte Buckland section). In that section he described fine micaceous schists with muscovite and biotite, above which there are several levels of conglomerate-agglomerate with clasts of schists and quartzose matrix. These conglomerates are interlayered with quartz-porphyry schists (the Tobífera Formation), which are in turn covered by slates and tuffs. Regarding the contact with the basal fine micaceous schists, Kranck (1932) stated that due to the strong deformation, it "*is as yet difficult to decide if the contact in question is a primary one, if there is a disconformity between the old schist of the Central-Cordillera and the quartz-porphyry formation, or if the contact is a tectonical one*" (p. 63). The strongest argument pointing towards an unconformity is the presence of conglomerates with clasts of schists, but the unconformity itself is not exposed.

Observations in Fiordo Relander and especially in Fiordo Finlandia led Kranck (1932) to conclude that the quartz-porphyry schists "*also occur in the inner parts of the Central-Cordillera in strongly metamorphic condition, and that it therefore is hardly possible to separate the old central schists (older than Monte Buckland Formation) and the fossil-bearing slates of the Monte Buckland series in these parts of the mountain range*" (p. 81). In summary, Kranck (1932) proposed an unconformity between the Tobífera Formation ("quartz porphyry schists" or Monte Buckland Formation) and the "high metamorphic schists", "central schists" or "old schists" of Cordillera Darwin, despite acknowledging that

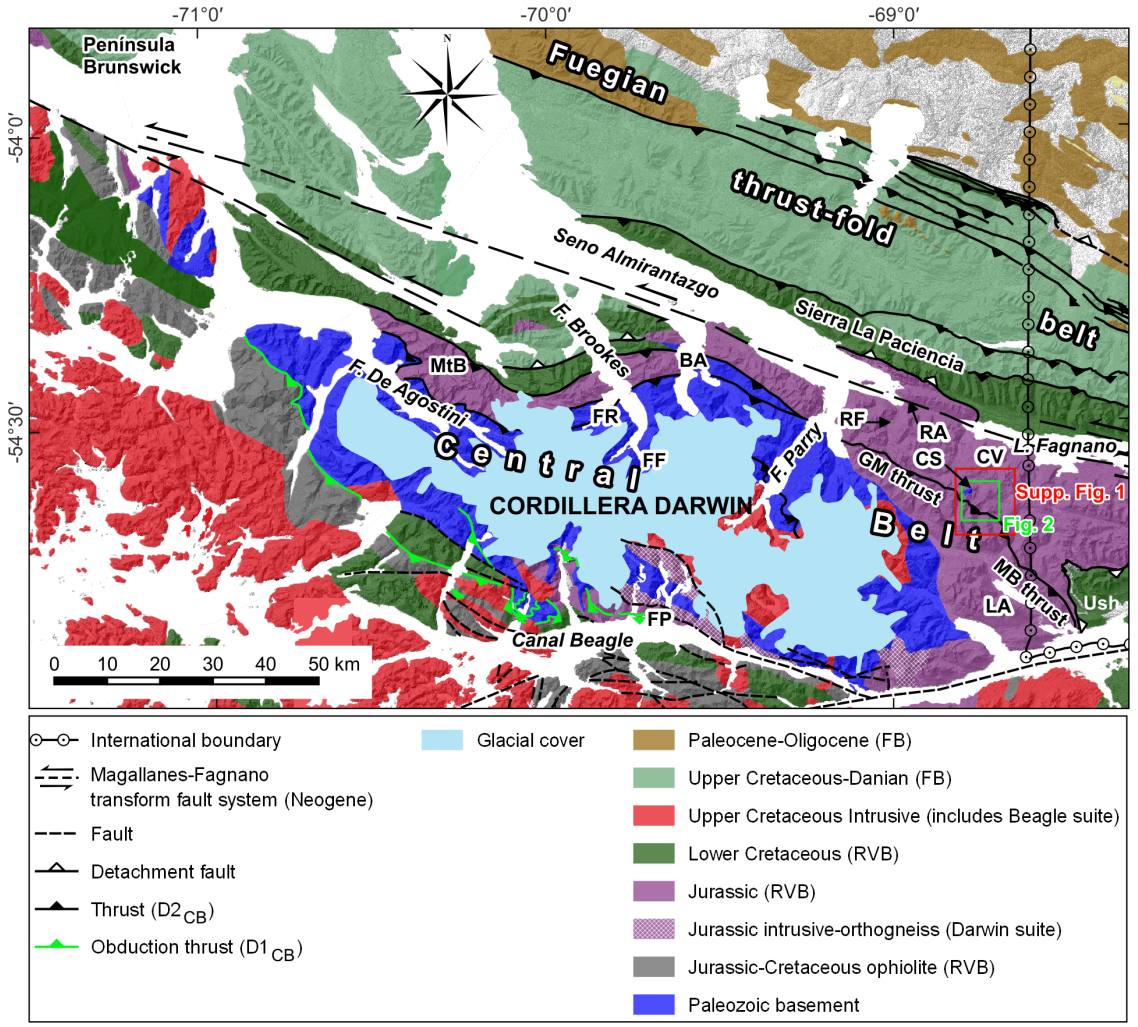

FIG. 1. Geological map of the central belt of the Fuegian Andes focused on Cordillera Darwin. Based on Sernageomin (2003), Hervé *et al.* (2010a), Klepeis *et al.* (2010), Cao *et al.* (2025), and Olivero *et al.* (2025). **FP**: Fiordo Pía, **CS**: Cerro Svea, **CV**: Cerro Verde, **FF**: Fiordo Finlandia, **GM**: Glaciar Marinelli, **MB**: Mina Beatriz, **MtB**: Monte Buckland, **LA**: Lago Acigami, **FR**: Fiordo Relander, **RA**: Río Azopardo, **RF**: Río Fontaine, **BA**: Bahía Ainsworth, **Ush**: Ushuaia, **FB**: Foreland Basin, **RVB**: Rocas Verdes Basin, $D1_{CB}$ and $D2_{CB}$ explained in text.

the contact between the two units was not clearly exposed, and that they were tectonically interleaved (pp. 114, 203-204).

It should be noted that even though he referred to the older unit as "high metamorphic schists", Kranck (1932) described no high-grade parageneses. Overall, the author assigned a greenschist facies to all these schists (*ibid.*, pp. 147-148).

In our study area, based on samples collected by P. Quensel in 1908, Kranck (1932) interpreted the same "highly metamorphic schists" described in the Central Cordillera (Kranck, 1932, p. 88). To the south, in the head of Lago Acigami (Roca), he mapped "schists of Lapataia" (pp. 93-95), which include metasedimentary rocks and greenschists of basic igneous protolith, interlayered with coarse conglomerate with clasts of deformed quartzitic schist, similar to conglomerates within the Tobífera Formation (Monte Buckland series) above the interpreted unconformity in the Monte Buckland section.

Much later, the work by Nelson *et al.* (1980) condensed the stratigraphic results of the few published

TABLE 1. SUMMARY OF PREVIOUS STRATIGRAPHIC WORK IN NORTHERN CORDILLERA DARWIN AND ADJACENT AREAS OF THE CENTRAL BELT (EXCLUDING LOWER CRETACEOUS METASEDIMENTARY ROCKS). SEE MORE EXHAUSTIVE DESCRIPTIONS IN THE TEXT.

Author(s)	Kranck (1932)	Cortés and Valenzuela (1960)	Nelson *et al.* (1980)		Johnson (1990)	Hervé *et al.* (2010)	Cao *et al.* (2022, 2025)	Mella and Quiroz (2023)
Area/locality	**Monte Buckland**	**Río Fontaine**	**Northern Cordillera Darwin**		**Bahía Ainsworth-Fiordo Brookes**	**Northern Cordillera Darwin**	**West of Ushuaia**	**Paso de las Lagunas, Cerro Svea**
Unit name *description*	**Monte Buckland Formation** *conglomerates, slates, tuffs*	**Río Fontaine Formation** *conglomerates, sandstones and slates*	**Cover Complex**	*Upper unit: volcaniclastic fine- to coarse-grained rocks*	**Seno Almirantazgo Volcanic-Sedimentary Complex** *volcanic, pyroclastic, sedimentary rock*	**Tobífera Formation (*cf.* Thomas, 1949)** from Permian to Middle Jurassic detrital zircon U-Pb ages	**Lemaire Complex** *volcanic-sedimentary complex Middle Jurassic-Berriasian zircon U-Pb ages*	**Tobífera Formation**
	Quartz-porphiry schists	**Porphyritic Series** *porphyries and slates*		*Lower unit: volcanic with basal clastic horizon*	**Basal Clastic Complex** *conglomerates, sandstones, slates*	(Increasing metamorphic grade)	**Lapataia Formation** *metapsamitic quartz-chlorite and quartz-sericite schists and phyllites metabasic greenstones-greenschists*	
	Unconformity		**Unconformity**		**Unconformity**	**Cordillera Darwin Metamorphic Complex** *includes Mesozoic cover and metasedimentites with Cambrian-Devonian detrital zircon U-Pb ages*		*Contact not exposed*
	High Metamorphic Schists or Old Schists *fine micaceous and quartzitic schists*		**Basement complex** *mostly metapelitic*		**Basement** *phyllites and schists (metapsamites) with chlorite, sericite, quartz, albite, calcite, epidote, amphibole, biotite, and garnet (contact metamorphism)*			**Estratos Paso de las Lagunas** *metaconglomerates and quartzites*
								Unconformity
								Cerro Svea granite *Late Devonian muscovite* $^{40}Ar/^{39}Ar$ *age*

and several unpublished studies in the region at that time. It also supported the existence in northern Cordillera Darwin of an unconformity between the "basement complex" and a "cover complex". Although their descriptions are not detailed, they maintained the characterization of the basement complex made by Kranck (1932) as essentially metapelitic rocks with minor amounts of quartzite and greenstone (basic metavolcanic rock). Nelson *et al.* (1980) also established a generalized cover succession that begins with a basal conglomerate with clasts of volcanic and basement rocks, the latter with inherited deformation fabrics. A silicic volcanic sequence with interlayered sedimentary horizons overlies this basal unit and is covered by volcaniclastic sedimentary rocks.

Johnson (1990) gave more detailed descriptions of the basal conglomeratic rocks, which he called "Basal Clastic Complex". This unit covers the basement with an inferred angular unconformity, or even by fault contact at some places. The coarse facies include clasts of phyllites and schists derived from the basement. Pyroclastic beds that form the base of the Seno Almirantazgo Volcanic-Sedimentary Complex conformably cover the Basal Clastic Complex, which is not evenly distributed since at some localities the tuffaceous deposits rest directly over the basement (without an exposed contact). More recent work included the Basal Clastic Complex and the Seno Almirantazgo Complex in the Tobífera Formation (Ortiz, 2007; Hervé *et al.*, 2010a). Johnson (1990) interpreted the semi-chaotic deposits of low textural and mineralogical maturity of the Basal Clastic Complex as rift deposits (avalanches), which incorporated eroded basement and clasts of the first volcanic products of the Rocas Verdes Basin. Descriptions of the basement unit made by Johnson (1990) are similar to those of Kranck (1932), emphasizing the metapsammitic protoliths of the schists and phyllites, and their greenschist facies metamorphic grade.

The only stratigraphic work in our study area, between Lago Fagnano and south of Paso de las Lagunas, is that of Klepeis (1994), discussed in more detail below. He recognized a major thrust fault (the "basement thrust"), which was thought to place "Paleozoic-Mesozoic basement schists" over the Lower Cretaceous La Paciencia Formation. Within the basement schists, Klepeis (1994) distinguished a felsic or siliceous facies, possibly metatuffs and meta-agglomerates, interlayered with more pelitic lithologies.

Later detailed analyses of the metamorphism in northern Cordillera Darwin confirmed no difference in metamorphic grade between the units mapped as basement and cover, ascribing the highest metamorphic grade to the Late Cretaceous orogeny (Kohn *et al.*, 1993; Ortiz, 2007). These works revealed that in the northern flank of Cordillera Darwin, greenschist facies index minerals are chlorite and biotite, with garnet restricted to the internal region. It was suggested that the basement unit was deformed before deposition of cover rocks, as indicated by the occurrence of deformed metamorphic rock fragments in the Basal Clastic Complex. This old deformation was attributed to early Mesozoic regional deformation in the margin of Gondwana (cf. Dalziel and Elliott, 1971), with two published Jurassic zircon U-Pb ages in granitic dikes cutting a prior foliation, constraining it as pre-Andean (Klepeis *et al.*, 2010; Hervé *et al.*, 2010a).

Recent research employing detailed petrographic descriptions, thermobarometric estimations and, more importantly, isotopic age determinations, has corroborated most of the descriptions of the basement and cover units. The most relevant stratigraphic update from this research is the definition of the Cordillera Darwin Metamorphic Complex, which includes both pre-Jurassic basement and Mesozoic cover rocks (Hervé *et al.*, 2010a).

It is important to recognize that the metasedimentary nature of both the basement and part of the cover hampers distinction between them in different maps (cf. Johnson, 1990; Ortiz, 2007; Hervé *et al.*, 2010a). The distinction is not always resolved by geochronological studies: Hervé *et al.* (2010a) found that rocks mapped as the Rocas Verdes Basin cover have prominent Paleozoic or older detrital zircon age peaks, while only a few grains (frequently less than 10) have Jurassic ages. This indicates a dominant detrital input from the basement, even within the volcanic-sedimentary complex of the Tobífera Formation, as shown elsewhere in the basin (Calderón *et al.*, 2007). This idea was recently used in redefinition of the age of the Lapataia Formation by Cao *et al.* (2022), which we address in more detail below.

Recently, Mella and Quiroz (2023) studied the Svea granite (Quensel, 1910) for which they reported a Late Devonian $^{40}Ar/^{39}Ar$ muscovite age, as well as an early Carboniferous $^{40}Ar/^{39}Ar$ muscovite age for an orthogneiss interpreted as a contact metamorphic product. They identified an unconformable cover to the Svea granite of quartzites and metaconglomerates,

which they named "Estratos Paso de las Lagunas", previously mapped as the Lower Cretaceous La Paciencia Formation by Klepeis (1994).

2.2.2. Stratigraphic synthesis

We now briefly describe an updated stratigraphic framework of the northern flank of Cordillera Darwin. Notice that various units from the pre-Jurassic basement to the Lower Cretaceous rocks were incorporated into the Cordillera Darwin Metamorphic Complex by Hervé *et al.* (2010a), as already mentioned. We describe them separately here.

Pre-Jurassic basement

This unit is composed of metasedimentary rocks and granitic intrusions. The metasedimentary components include phyllites and fine schists, with quartz, muscovite, biotite, chlorite, and epidote. They are derived from fine-grained sedimentary rocks. A subordinate facies of greenstones or greenschists, with more abundant chlorite, epidote and amphibole, is possibly derived from basic igneous rocks (Kranck, 1932). The metamorphic grade of these rocks is within the greenschist facies, mostly within the chlorite and biotite isograds. Only at the heads of Fiordo Brookes and Fiordo Parry are these rocks within the garnet isograd, close to granitic intrusions and along with the higher-grade metamorphic zone of Cordillera Darwin (Kranck, 1932; Kohn *et al.*, 1993, 1995; Ortiz, 2007). The mostly buried contact with the Rocas Verdes Basin cover is an interpreted unconformity that has never been described precisely.

Granitic intrusions of the basement include the Devonian Svea granite, overprinted by an episode of early Carboniferous metamorphism (Mella and Quiroz, 2023). This rock is unconformably covered by the Estratos Paso de las Lagunas (see above). No other granite of Paleozoic age is known from the study area. However, recent findings in Argentina indicate the presence of exhumed Paleozoic granitic basement in the horsts of Jurassic hemigrabens, unconformably covered by sedimentary and tuffaceous facies of the Lemaire Complex (Lobo *et al.*, 2024). Also, Paleozoic granites have been cored in the subsurface of the Austral-Magallanes basin in northern Tierra del Fuego (Söllner *et al.*, 2000; Hervé *et al.*, 2010b; Castillo *et al.*, 2017; de la Cal *et al.*, 2023).

Hervé *et al.* (2010a) provided several detrital zircon U-Pb ages from schists of the Cordillera Darwin Metamorphic Complex that may be considered part of the pre-Jurassic basement, especially (according to those authors) samples with Carboniferous youngest zircon ages, and Devonian, Ordovician, Cambrian and older age peaks. We will discuss these results in more detail in this work.

Lapataia Formation. Jurassic

The Lapataia Formation has its type area at the southwestern corner of Argentine Tierra del Fuego, cropping out in a ~10 km wide belt east of the international boundary. It extends into Chilean territory along the head of Lago Acigami; according to Kranck (1932), similar rocks are exposed between this lake and Paso de las Lagunas. In the type area the Lapataia Formation is thrust onto the Lemaire Complex, and its base and thickness are unknown.

The Lapataia Formation consists of a metasedimentary facies of phyllites and very fine schists with quartz, muscovite, chlorite and minor biotite, and a metabasic facies formed by greenschists and greenstones (Cao *et al.*, 2018, 2022). The metasedimentary facies reveals primary sedimentary layering, formed by an alternation of quartzite layers and metapelitic layers with muscovite, chlorite and occasional biotite porphyroblasts. The sedimentary layering is transposed by the dominant tectonic foliation, formed during $D1_{CB}$ (Cao *et al.*, 2018; Torres Carbonell *et al.*, 2020). The metabasites represent a basic volcanic or pyroclastic protolith, and are distinguished by abundant epidote and tremolite-actinolite.

Four samples from the coarsest horizons of the metasedimentary facies gave several Paleozoic detrital zircon U-Pb ages, with none younger than Permian (Cao *et al.*, 2022). A thorough structural and petrographic examination of the rock showed no tectonic deformation older than Late Cretaceous $D1_{CB}$, but revealed clasts of foliated metamorphic rocks with an inherited deformation, which led Cao *et al.* (2018, 2022) to interpret this unit as part of the cover of the Rocas Verdes Basin with a possible Jurassic age. It therefore represents the deposits of the early rifting during opening of the basin, with abundant detritus supplied from eroded basement highs. Cao *et al.* (2022) concurred with Hervé *et al.* (2010a) in considering that the absence of Jurassic zircons cannot be solely used to assess the depositional age of these rocks, especially when they lack coeval volcanic material. We will further discuss this aspect in section 5.2.

Tobífera Formation-Lemaire Complex. Middle Jurassic-Berriasian

The Tobífera Formation was defined from subsurface data in northern Tierra del Fuego and includes exposures of mainly silicic volcanic and associated rocks along the southern Patagonian and Fuegian Andes (Thomas, 1949). Studies in Tierra del Fuego recognized acidic and less abundant basic volcanic rocks, several pyroclastic facies, and associated volcaniclastic and marine sedimentary deposits, accumulated during the rifting that affected this portion of Gondwana in the Jurassic (Cortés and Valenzuela, 1960; Dalziel *et al.*, 1974; Bruhn *et al.*, 1978; Johnson, 1990; Hanson and Wilson, 1991; González Guillot *et al.*, 2016; Cao *et al.*, 2022). This unit is more easily recognized in outcrops when it consists of felsic porphyries (cf. Kranck, 1932), but generates confusion when represented by metasedimentary facies, especially in highly deformed zones where these rocks are interlayered with the supposed basement schists (*e.g.*, at Fiordo Relander and Fiordo Finlandia; cf. Kranck, 1932; Ortiz, 2007). The inclusion of the Basal Clastic Complex of Johnson (1990) as an integral part of the Tobífera Formation (cf. Ortiz, 2007; Hervé *et al.*, 2010a) adds a variety of clastic facies to this volcano-sedimentary complex, with an importance within the sequence that is usually minimized. In fact, this coarse-grained succession is usually ascribed to the base of the formation mainly due to description of isolated outcrops in the Monte Buckland section, and at Fiordo Brookes, Bahía Ainsworth, and Fiordo Parry. However, there are also similar coarse-grained horizons at intermediate positions within the Tobífera Formation (Johnson, 1990), including the succession distinguished by Cortés and Valenzuela (1960) as the Río Fontaine Formation in the eponymous river (see Table 1). Also, several conglomerate and sandstone horizons and lenses are known from the equivalent Lemaire Complex in Argentina (see Cao *et al.*, 2025 for a review).

The age of the Tobífera Formation-Lemaire Complex is constrained from dating of the volcanic and volcaniclastic horizons with U-Pb zircon ages that range from Middle Jurassic to Berriasian (Calderón *et al.*, 2007; Hervé *et al.*, 2010a; Palotti *et al.*, 2012; Cao *et al.*, 2025). These ages, however, are restricted to facies with a prominent acidic volcanic composition, such as rhyolites and ignimbrites. In other horizons where a tuffaceous composition is not dominant, recycled Paleozoic detrital zircons are more abundant. For example, Hervé *et al.* (2010a) reported detrital zircon U-Pb ages from samples within the Tobífera Formation sedimentary horizons in Cordillera Darwin. One sample (FO0524) gave Early Triassic ages and a prominent Cambrian age peak, but no Jurassic ages. Another sample (FO0539) gave a prominent Carboniferous age peak and only two grains (three SHRIMP spots) with Middle Jurassic ages. Finally, a granodiorite clast near the base of the Tobífera Formation at Fiordo Parry (sample FO0516) has an Ordovician crystallization age. More significantly, sample FO0508, mapped as basement in an amphibolitic schist with garnet and biotite, has a prominent Devonian age peak but six grains (eight spots) record Middle Jurassic ages. Otherwise, in the absence of Jurassic grains, Hervé *et al.* (2010a) proposed as a working hypothesis that samples with Permian or Triassic ages could be considered part of the cover. However, samples that possibly belong to the cover also have older detrital zircon ages. This highlights the problem studied by Cao *et al.* (2022) in the Lapataia Formation, mentioned above, which applies similarly to the Tobífera Formation. Below, we will compare in detail some of the samples mentioned here with our data.

Granites of the Darwin suite exposed in southern Cordillera Darwin have been associated genetically with the Tobífera Formation (Hervé *et al.*, 1981). These have U-Pb zircon crystallization ages between Middle and Late Jurassic (Mukasa and Dalziel, 1996; Klepeis *et al.*, 2010).

Río Jackson and La Paciencia Formations. Lower Cretaceous

Slates and shales of the La Paciencia Formation crop out in the northern flank of Cordillera Darwin at Fiordo Brookes and Bahía Ainsworth, where the contact with the older Tobífera Formation is tectonic. The La Paciencia Formation was defined north of Lago Fagnano, where it contains Cretaceous fossils (Cortés and Valenzuela, 1960). Towards the east, in Argentina, it corresponds to the Beauvoir Formation, with Aptian-Albian invertebrates and consistent U-Pb detrital zircon ages near its base (Olivero *et al.*, 2009; Martinioni *et al.*, 2013; Cao *et al.*, 2025). These mostly fine-grained sedimentary and metasedimentary rocks contain abundant thin intercalations of tuffaceous horizons, usually a few centimetres thick. North of Lago Fagnano, the La Paciencia Formation conformably rests on a relatively thin horizon

(less than 100 m thick) of intercalated shales, marls, and fossiliferous limestone, known as the Río Jackson Formation (Cortés and Valenzuela, 1960). This latter formation lies over the Tobífera Formation with a tectonic contact (thrust detachment; Klepeis, 1994).

Klepeis (1994) mapped the Río Jackson and La Paciencia formations south of Lago Fagnano, in a NW-SE belt between Cerro Verde and Cerro Svea. Some of these rocks were included in the previously mentioned Estratos Paso de las Lagunas by Mella and Quiroz (2023). These rocks are one of the main topics of study in this work, and will be addressed below.

Late Cretaceous Beagle Suite

The youngest intrusive rocks cropping out in northern Cordillera Darwin comprise some diorite stocks and dikes affecting the Cerro Matrero Formation in the northern area of Fiordo Brookes (Johnson, 1990), and granitic intrusives mapped at Fiordo Parry and south of Cerro Svea (Nelson *et al.*, 1980; Johnson, 1990; Hervé *et al.*, 2010a; Klepeis *et al.*, 2010). Both the Darwin and Beagle suites crop out in the inner portion of Fiordo Parry (Nelson *et al.*, 1980; Ortiz, 2007; Hervé *et al.*, 2010a; Klepeis *et al.*, 2010). Klepeis (1994) mapped a possible granite south of Cerro Svea, which has not been studied in detail.

2.3. Previous structural work

Several previous studies highlighted the structural complexity of Cordillera Darwin (Nelson *et al.*, 1980; Dalziel and Brown, 1989; Klepeis, 1994; Klepeis *et al.*, 2010; Betka *et al.*, 2022). We will restrict our analysis of previous research to the area directly relevant to our work, in northern Cordillera Darwin, which includes the work of Nelson *et al.* (1980) and Klepeis (1994). Similar work directly east of this area, in Argentina, was performed by Bruhn (1979) and later by Cao *et al.* (2018, 2023). A comparison of the generations of regionally recognized structures is given in table 2, while the regional tectonic context is discussed by Torres Carbonell *et al.* (2020) and Cao *et al.* (2023).

Nelson *et al.* (1980) established a regional deformation sequence that starts with a pre-Jurassic deformation of the basement (Db; see Table 2), which was not clearly distinguished from younger structures, was not illustrated in detail, and seems to be inferred from the occurrence of foliated rock fragments in conglomerates of the Tobífera Formation. The first "Andean" deformation distinguished by Nelson *et al.* (1980) is a "strongly developed foliation" that is more intense in southern Cordillera Darwin. In northern Cordillera Darwin (but west of our study area), this deformation is a slaty cleavage at high angles to bedding and axial-planar to open folds. In the basement unit (it is not clear if this refers to northern or southern areas) it is a phyllitic or schistose foliation in pelitic lithologies, axial-planar to tight or isoclinal folds in siliceous rocks. This foliation, called S1 by Nelson *et al.* (1980), has associated stretching and intersection lineations called L1.

The subsequent structural generation described by Nelson *et al.* (1980) differs between the northern and southern areas of Cordillera Darwin. To the south, it is a complex set of macroscopic and mesoscopic folds and axial-planar cleavage (S2), which fold previous S1 surfaces and were formed during peak metamorphic conditions. Metamorphic porphyroblasts such as staurolite and large amphiboles grew coevally with the S2 foliation. However, in our area of interest in northern Cordillera Darwin, Nelson *et al.* (1980) described S2 as an anastomosed phyllitic cleavage that intersects S1 at low angle, in a way "*similar to shear fracture cleavages (SF-tectonite fabrics)*" (p. 738). We emphasize that these terms (fracture cleavage, SF-tectonite) are now anachronistic, but refer to spaced foliations, and possibly foliated cataclasites. The spaced foliation associated with brittle or brittle-ductile structures is clearly different from the S2 cleavages formed during the staurolite-grade metamorphism in southern Cordillera Darwin. The spaced S2 foliation described by Nelson *et al.* (1980) in northern Cordillera Darwin is the youngest structure that they recognized in this area, since their D3 deformation is restricted to southwestern Cordillera Darwin.

The work of Nelson *et al.* (1980) constituted the cornerstone for subsequent structural work in the region, including the detailed mapping by Klepeis (1994), who interpreted a NW-SE belt of Lower Cretaceous rocks (Río Jackson and La Paciencia formations) between Cerro Verde and south of Paso de las Lagunas (see Klepeis' original map in Supplementary File 1). The southern boundary of this belt is a thrust, interpreted as carrying the Paleozoic basement over the Lower Cretaceous rocks ("basement thrust" in Klepeis, 1994). In a more recent work this

TABLE 2. CORRELATION OF STRUCTURAL FABRICS DESCRIBED IN NORTHERN CORDILLERA DARWIN (EXCLUDING OTHER AREAS) BY PREVIOUS WORK AND IN THIS STUDY, AND THEIR TECTONIC INTERPRETATION. SEE DETAILED DESCRIPTIONS IN THE TEXT.

Tectonic stage	Author and nomenclature		
	Nelson *et al.* (1980)	**Klepeis (1994)**	**This work**
Pre-Jurassic deformation in the SW margin of Gondwana	Db, mostly inferred from deformed-foliated clasts in Jurassic rocks	Hanging wall of the Glaciar Marinelli Thrust: S1, "an early foliation observed mainly in thin section", subparallel to quartz veins	**No pre-Jurassic tectonic fabric**
Late Cretaceous closure of the RVB NE-directed obduction of RVB floor and cover, and SW-directed underthrusting of contiental margin, culminating in arc-continent collision(Bruhn, 1979; Nelson *et al.*, 1980; Cunnigham, 1995; Kohn *et al., 1995;* Klepeis *et al., 2010;* Maloney *et al.*, 2011; Betka *et al.*, 2015, 2022). **D1CB deformation in Torres Carbonell *et al.* (2020)**	**D1** In northwest Cordillera Darwin: S1, slaty cleavage axial-planar to open folds L1, associated stretching and intersection lineations	Footwall of Glaciar Marinelli Thrust: S1, "dominant foliation", fine spaced cleavage, cuts sedimentary lamination (S0) L1, downdip mineral lineation on S1 surfaces Hanging wall of the Glaciar Marinelli Thrust: F2, isoclinal folds deforming the S1 early foliation S2, "dominant" foliation, "crenulation cleavage", axial-planar with the F2 folds, coplanar with the footwall S1 L2, downdip stretching lineation on S2	S0 (Jurassic), in the hanging wall of the Glaciar Marinelli Thrust is distinguished as metapsammite (quartz-feldespathic) and metapelite (sericite-chlorite) bands, parallel to quartz veins, and partially transposed by S1 S1, main penetrative foliation in the study area, with stretching lineation L1 Transposed S0 forms rootless F1 folds in the more strained zones
Deformation after arc-continent collision with NE-directed thrusting and formation of the Fuegian thrust-fold belt, emplacement of thrust sheets and propagation of deformation to the foreland during the Paleogene to early Neogene. Final exhumation of the central belt (Álvarez Marrón *et al.*, 1993; Klepeis and Austin, 1997; Klepeis *et al.*, 2010; Torres Carbonell *et al.*, 2020; Cao *et al.*, 2023). **D2CB deformation in Torres Carbonell *et al.* (2020)**	**D2** In northern Cordillera Darwin: S2, spaced foliation associated with brittle or brittle-ductile structures	Footwall of Glaciar Marinelli Thurst: S2, fine spaced cleavage at low angle to S1 S3, crenulation cleavage that deforms S1 and S2, best development near the Glaciar Marinelli thrust F4, broad and open minor folds, developed on S3 and earlier fabrics Hanging wall of the Glaciar Marinelli Thrust: S3, crenulation foliation, with associated small folds (F3) S3 is deformed by shear bands, with usual top-to-NE shear sense F4, folds in the previous fabrics associated with these shear bands	S2, crenulation foliation best developed near brittle-ductile thrust zones L2, crenulation lineation (intersection of S1 and S2) Associated macroscopic deformation forms F2 folds in close relationship with shear bands

has been called the Glaciar Marinelli Thrust (Rojas and Mpodozis, 2006).

Klepeis (1994) described structures above and below this major thrust, using labelling that cannot be directly correlated across it (*e.g.,* S1 in the hanging wall is older and different from S1 in the footwall). In the footwall, Klepeis (1994) described the structures shown in table 2. The "dominant foliation" (S1) is a penetrative, finely spaced cleavage defined by aligned muscovite and chlorite and anastomosed pressure-solution seams, with flattened feldspars and dynamically recrystallized quartz in the microlithons. This foliation cuts the recognized sedimentary lamination (S0) at a low angle. A penetrative downdip mineral lineation (L1) is distinguished on S1 surfaces and is formed by the preferred alignment of flattened porphyroclasts and muscovite.

A second structure mentioned by Klepeis (1994) is a "*fine spaced cleavage at low angle to S1*", which dips to the south or west, and is called S2. He gave no further detail about this structure.

Finally, Klepeis (1994) described a "*moderately dipping crenulation cleavage that deforms S1 and S2*", called S3. This structure is not as conspicuous as S1, with its best development near the Glaciar Marinelli Thrust. Broad and open minor folds (F4) are developed on earlier fabrics. Klepeis (1994) interpreted S1, L1, and S2 in the footwall of the Glaciar Marinelli Thrust as equivalent to S1, L1, and S2 as described by Nelson *et al*. (1980) in northern Cordillera Darwin (see Table 2).

In the hanging wall of the Glaciar Marinelli Thrust, Klepeis (1994) described "*an early foliation observed mainly in thin section*", also labelled S1. This foliation is defined by the preferred orientation of aligned muscovite and chlorite, quartz aggregates and pressure-solution seams. It is subparallel to quartz veins and is deformed into isoclinal folds together with them (F2).

According to Klepeis (1994), the "dominant" foliation in the Glaciar Marinelli Thrust hanging wall is "*an intensely penetrative crenulation cleavage*" that overprints S1, and is called S2 (Table 2). This cleavage is defined by pressure-solution seams and "new" chlorite and muscovite, and is axial-planar with the F2 folds. Remarkably, this S2 in the hanging wall is coplanar with the S1 in the footwall of the thrust. S2 has an associated downdip stretching lineation (L2), defined by stretched and recrystallized quartz porphyroclasts.

S2 in the hanging wall is crenulated by a third foliation enhanced by pressure-solution seams, called S3 by Klepeis (1994), with associated small, tight and upright folds (F3). This S3 crenulation is deformed by low-angle shear bands with gentle dips, both to the south and north. Broad, open folds in the previous foliations (F4) are associated with development of these shear bands, with usual top-to-northeast shear sense.

The overprinting relationships interpreted by Klepeis (1994) led him to correlate S1 in the hanging wall with the Db deformation of Nelson *et al.* (1980), and his "dominant foliation" S2 with the dominant fabric in basement rocks of Nelson *et al.* (1980), which they called S1 (see Table 2). Accordingly, S3 would correspond to S2 of Nelson *et al*. (1980).

3. Methods

Fieldwork in the study area (Fig. 2) was focused on mapping of lithologies and structures. We collected orientated samples for microstructural and petrographic studies on sites shown on the map. Samples CD05 and CD06 were collected for U-Pb dating of detrital zircons (locations given in Supplementary File 2). Sample CD05 is a metasedimentary phyllite in the hanging wall of the Glaciar Marinelli Thrust, a unit mapped as Paleozoic-Mesozoic basement by Klepeis (1994; see Supplementary File 1). Sample CD06 is a metapsammite intercalated with breccias and dark slates at Paso de las Lagunas, which was mapped by Klepeis (1994) as La Paciencia Formation (see Supplementary File 1), and by Mella and Quiroz (2023) as Estratos Paso de las Lagunas.

Both samples were analysed for geochronology at the GeOHeLiS platform, University of Rennes (France) by laser ablation inductively coupled plasma mass spectrometry (LA-ICP-MS). The detailed analytical methods are explained in Supplementary Files 3 and 4, and results are listed in Supplementary File 2. Only 90-110% concordant data were used. Single-grain concordia ages according to Vermeesch (2021a) were calculated using *IsoplotR* (Vermeesch, 2018); these were only used for the kernel density estimation (KDE) diagrams, all the rest of the ages mentioned in the text are apparent ages ($^{206}Pb/^{238}U$ when age <1000 Ma, else $^{207}Pb/^{206}Pb$) or calculations derived from them. The maximum depositional ages are reported as the weighted mean of the youngest three zircons with overlapping 2σ uncertainty (Y3Go),

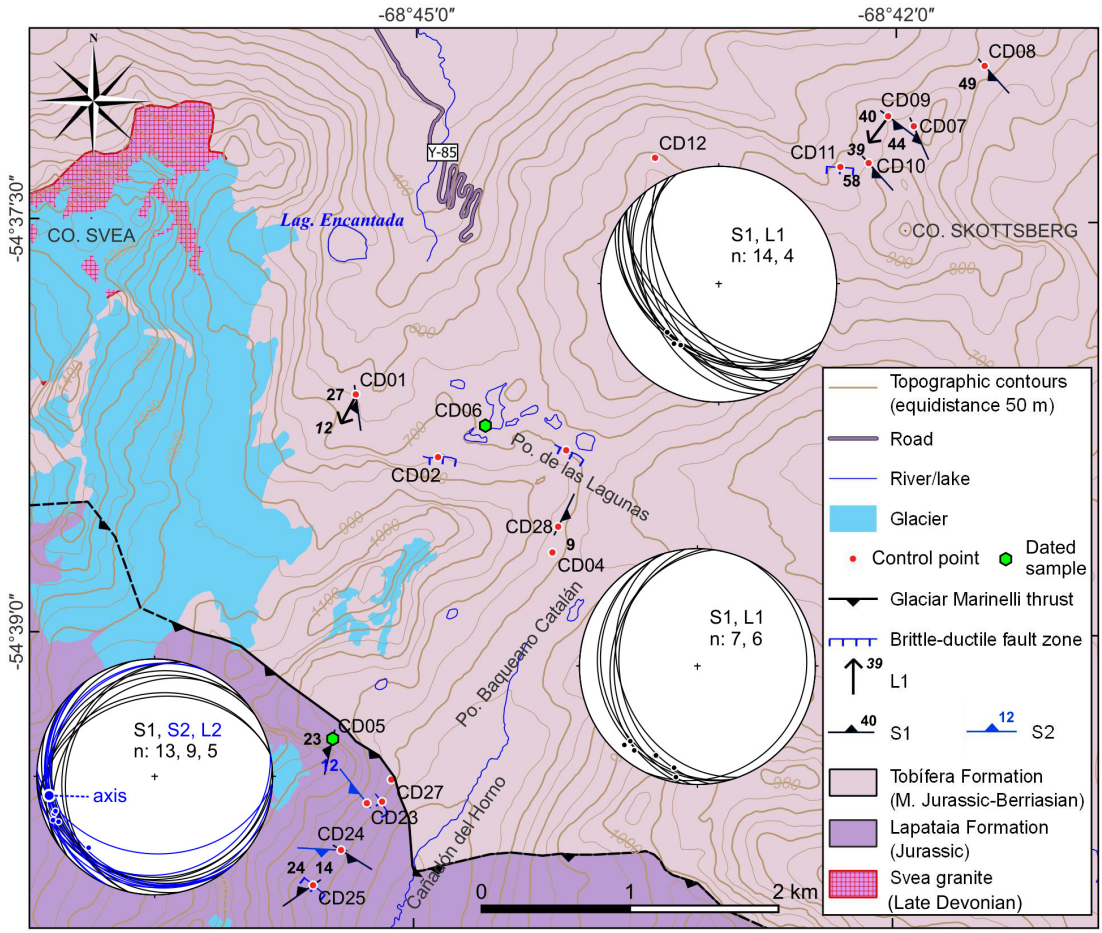

FIG. 2. Geological map of the studied area, with main structural features and stratigraphy based on our results (located in Fig. 1). Boundaries of the Svea granite are from Mella and Quiroz (2023). Small numbers are dips/inclinations in degrees. The spherical projections are equal-area, lower hemisphere for the areas of Cerro Skottsberg, Paso de las Lagunas, and the hanging wall of the Glaciar Marinelli Thrust. They show planes (great circles) and lineations (small dots) as indicated (black: S1, L1; blue: S2, L2), with n: number of measurements. The axis marked in the Glaciar Marinelli Thrust hanging wall is the theoretical mean folding axis calculated from folded S1 surfaces.

following the criteria suggested by Dickinson and Gehrels (2009), Coutts *et al.* (2019), Copeland (2020), and Sharman and Malkowski (2020). We also report the age of the youngest single grain (YSG) and the maximum likelihood (MLA) method of Vermeesch (2021b). Single-grain concordia age and MLA errors are reported as 2σ, whilst for the Y3Go and YSG ages errors are 2se.

All structural and microstructural descriptions made here follow terminologies stated by Passchier and Trouw (2005) and Twiss and Moores (2007). We used *Stereonet* software from R.W. Allmendinger to plot equal-area spherical projections of structural data.

4. Results

4.1. Field geology and petrography

We describe in this section the lithological and structural relationships at both outcrop and microscopic scale, as observed in two areas (Fig. 2): 1) between the Glaciar Marinelli Thrust and the northern flank of Cerro Skottsberg (footwall of this thrust), and 2) the western flank of Cañadón del Horno (hanging wall).

4.1.1. Footwall of the Glaciar Marinelli Thrust

The rocks exposed here include intercalated rhyolite, chloritic fine-grained schists (tuffs), schistose

breccias, metapsammites, and slates. The contacts between these facies are usually obliterated or very difficult to distinguish due to intense deformation. The rhyolite crops out at CD08 (Fig. 3A; see locations in figure 2), intercalated with chloritic schists with deformed or unexposed contacts, and develops a rough disjunctive foliation, which dips moderately to the SW (Fig. 2). Under the microscope (Fig. 3B), the rhyolite has porphyritic texture, with a fine-grained felsitic groundmass revealing devitrification (spherulitic texture). Fine-grained sericite is orientated, forming rough cleavage domains with variable spacing, and microlithons with weakly orientated fabric. Pressure-solution seams also define the cleavage domains. Phenocrysts are variably sized quartz, subhedral-to-euhedral plagioclase and sanidine, and glomerocrysts formed by these three species. Individual quartz crystals are anhedral or euhedral with perfect hexagonal habits, as well as embayments and slight deformation features (lamellae, undulose extinction and subgrain development). Accessory minerals include zircon, allanite and biotite, completely replaced by pseudomorphic chlorite. Epidote and chlorite comprise the main metamorphic minerals. The modal classification is a rhyodacite with 15% alkali-feldspar, 41% plagioclase and 44% quartz.

The intercalated chloritic schists (Fig. 3C) have a conspicuous green coloration in outcrop and are frequently cut by quartz veins. They have a very well-developed cleavage and a stretching lineation in cleavage planes. Typical exposures are those seen at CD07 and CD09. Under the microscope, alternating bands of chlorite and quartz-sericite form the cleavage, which surrounds deformed porphyroclasts of plagioclase, alkali-feldspar and minor quartz, and volcanic rock fragments with devitrified groundmass. Plagioclase crystals are deformed, stretched, and in general altered to sericite and epidote. Quartz porphyroclasts reveal embayments. The chloritic bands are probably derived from altered pumiceous horizons and are associated with abundant euhedral epidote in aggregated prismatic crystals, mostly pistacite. These aggregates have variable sizes but reach up to 200 µm, and in general replace plagioclase. The quartz-sericite bands are formed by a very fine mass of quartz, feldspars and abundant sericite, with minor chlorite. The quartzo-feldspathic material has grain-shape preferred orientation parallel to the foliation dipping moderately SW, revealing incipient bulging in quartz. Metamorphic minerals comprise chlorite, epidote, sericite, quartz, and calcite.

The breccias (Fig. 3D) consist of angular clasts of acidic volcanic rock (dominantly), with sizes from a few millimetres to more than 6 cm, in a very fine or sandy matrix that bears a finely spaced foliation. These rocks crop out at several places (*e.g.*, CD12), and conspicuously in the area of Paso de las Lagunas and Paso Baqueano Catalán, where they are intercalated with metapsammites, slates and micaceous-chloritic phyllites. The breccias have abundant matrix and variable amounts of clasts of quartz and feldspars, and rock fragments (volcanic rock, slate, granite), mostly angular and with poor sorting. The clasts are usually highly flattened and stretched; at some outcrops (*e.g.*, CD28), cigar-shaped clasts form part of a fabric that resembles L- or SL-tectonites.

Microscopic examination of the finer breccias reveals large clasts of very coarse sand or gravel immersed in an abundant (>30%) matrix. The matrix is formed by coarse sandstone and abundant very fine sand and silt, overprinted by very fine metamorphic sericite. Orientated sericite and flattened and stretched clasts, surrounded by anastomosed pressure-solution seams, define the tectonic foliation, which is closely spaced (micro-disjunctive) in the finer matrix. The microlithons in this fine matrix are weakly to completely orientated (Fig. 3E, F). A younger superposed foliation, formed by a zonal crenulation, is developed in the finer grained or micaceous parts of the sample (*e.g.* within metapelitic clasts), especially near thrust zones (see below).

Clasts are angular or subangular-to-subrounded, formed dominantly by quartz, feldspars, and fragments of volcanic or sedimentary rock. The volcanic rock fragments are either felsitic or mafic groundmass, the latter with very fine chlorite, epidote and plagioclase. The sedimentary rock fragments are pelitic, with very fine metamorphic sericite orientated parallel to the tectonic foliation. Less abundant components include metamorphic rock fragments. We highlight the occurrence of clasts of metamorphic rocks with an inherited foliation, in some cases oblique to the foliation in the breccia. Some of these are fine-grained metasedimentary rock formed by aligned sericite and muscovite, and others fine schists of granoblastic quartz and micas (Fig. 3E, F). Additional clasts with phaneritic granoblastic texture containing perthitic feldspar and quartz, and euhedral muscovite, may be acid igneous intrusive rock fragments such as

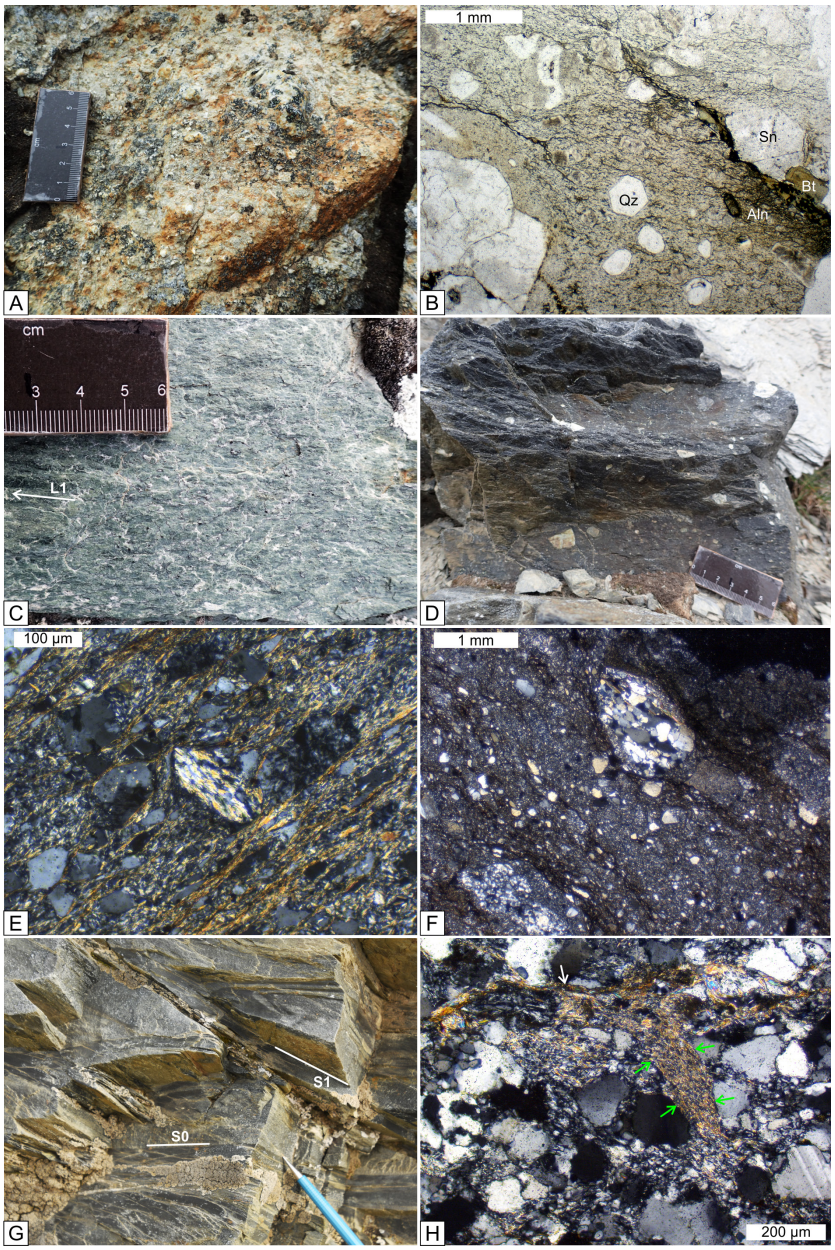

FIG. 3. **A.** Rhyolite from point CD08, showing porphyritic texture with quartz and feldspar phenocrysts in an aphanitic groundmass. **B.** Photomicrograph (plane-polarized light, PPL) of the same rhyolite with phenocrysts of quartz (Qz), sanidine (Sn) and biotite (Bt). Aln is allanite. Cleavage is NW-SE in the photo (pressure-solution seams). **C.** Chloritic fine-grained schist (CD09) with well-developed cleavage (in plane of photograph) and a stretching lineation (L1) formed by deformed clasts. **D.** Breccia with pebble-sized clasts, mainly of felsic volcanic rocks (CD12). **E.** Photomicrograph (cross-polarized light, CPL) of the breccia shown in D, note foliated clast with an inherited fabric oblique to the NE-SW foliation in the breccia. **F.** Photomicrograph (CPL) of a breccia (CD28) with a clast of foliated metamorphic rock (above center), formed by granoblastic quartz with grain-shape preferred orientation and orientated biotite, contrasting with the disjunctive anastomosed foliation in the breccia matrix. The latter (NW to SE) consists mostly of pressure-solution seams with only very fine metamorphic sericite in the finer fraction. **G.** Metapsammites from CD10, with well-defined layering (S0) and finely spaced cleavage (S1), as well as very tight folds in S0 (upper part of photograph). **H.** Photomicrograph (CPL) of sample CD06, with a foliated metamorphic clast (green arrows). The fine continuous foliation in the clast contrasts with the rough disjunctive foliation in the matrix, which runs horizontally and is marked by pressure-solution seams, flattened and stretched detrital micas (*e.g.*, white arrow) and fine metamorphic sericite.

granite. Frequent flattened and stretched fragments of crystalline chlorite and anhedral quartz are probably altered pumice. Detrital muscovite is also present. Minor components include titanite, zircon, and detrital biotite with pseudomorphic replacement by chlorite.

The metapsammites and slates form extensive outcrops interfingered with the other facies. In the slates and phyllites, the stratification is usually transposed by the main cleavage, with development of a distinct stretching lineation (Fig. 4A, B). In the northeastern portion of our map area the foliation dips consistently SW (Fig. 2), but towards Paso de las Lagunas the foliation has a more northerly strike, with dominant westward low-angle dips. The stretching lineation plunges SW. Metapsammites have a well-developed spaced foliation, anastomosed in the coarser facies, and axial-planar to tight folds (sample CD10; Fig. 3G). The slates characteristically reveal stretched and flattened ellipsoidal pyroclastic fragments, resembling altered accretionary pellets.

Under the microscope, the metapsammites reveal poorly sorted angular-subangular clasts up to 0.4 mm. The matrix is coarse silt with abundant metamorphic chlorite and sericite. The sand clasts have sutured or lobate boundaries, with no visible pores between them. The main components are quartz, sericitized plagioclase, and alkali-feldspar with partial albitization. Subordinate components are metamorphic rock fragments with granoblastic texture (quartz with subgrain rotation recrystallization) and metasedimentary rock fragments that reveal a fine continuous foliation. Even though many of these clasts are flattened and orientated parallel to the cleavage in the metapsammites, some of them evidence a pre-existing tectonic foliation (sample CD06; Fig. 3H). There are minor amounts of detrital muscovite and altered biotite, usually flattened between more competent grains. Some muscovite grains have a magmatic or metamorphic origin, as revealed by their inclusion into granoblastic polycrystalline quartzo-feldspathic fragments. Titanite and zircon are present as accessory minerals. Modal determinations in two samples reveal 26% and 12% alkali-feldspar, 33% and 50% plagioclase, 41% and 36% quartz, and 2% metasedimentary rock.

The disjunctive foliation in the metapsammites is variably developed, formed by anastomosed pressure-solution seams and abundant orientated fine sericite and quartz, both replacing the sedimentary matrix and forming strain fringes and necks in microboudinaged clasts. Orientated, very fine biotite or stilpnomelane also form in the cleavage domains. Very fine disseminated epidote and less-frequent calcite complete the metamorphic paragenesis.

The dominant structural fabric in the footwall of the Glaciar Marinelli Thrust is a tectonic foliation defined by the grain-shape preferred orientation of porphyroclasts, orientated metamorphic minerals such as sericite and chlorite, and pressure-solution seams (Figs. 3 and 4). Macroscopically, this foliation is clearly distinguished as a schistosity in the less-competent rocks, but is not as well developed in competent rocks such as cemented sandstones and rhyolite. In the less competent metasedimentary rocks, the foliation transposes the original sedimentary layering (*e.g.*, Fig. 4A). In intensely deformed horizons, stretched porphyroclasts and metamorphic phyllosilicates are orientated such that they form a stretching lineation (Fig. 4B). We label this foliation S1, and the stretching lineation L1. We find both fabrics comparable to foliation S1 and lineation L1 of Klepeis (1994) in the footwall domain, and with S1 and L1 mapped by Nelson *et al.* (1980) in northern Cordillera Darwin (Table 2). Away from the Glaciar Marinelli Thrust, near Cerro Skottsberg, S1 has a NW-SE strike and dips moderately SW, being subparallel to the tectonic grain in the region. Towards the Glaciar Marinelli Thrust, S1 seems to be tilted by major folding, with a near N-S strike and gentle dips either to the west (mostly) or east. Folding of S1 is evident near or within shear zones, as described below.

Brittle-ductile thrusts are frequent in the footwall domain, characterized by fault zones several metres thick (Fig. 4C), orientated from ENE-WSW to ESE-WNW. Shear sense indicators such as deflected sigmoidal S1 foliation along shear bands reveal consistent top-to-north kinematics (Fig. 4D, E). These deflections, as well as asymmetric folds of the S1 foliation (Fig. 4F, G), are conspicuous within and near the brittle-ductile fault zones, and are dominantly orientated parallel to these zones, with variable hinge attitudes. Towards the Glaciar Marinelli Thrust, this folding of S1 surfaces is more intense and manifests microscopically as a zonal crenulation cleavage, which constitutes a macroscopic smooth to anastomosed spaced foliation with crenulation folds visible in the microlithons (Fig. 4H). This foliation is labelled S2 in this work and is comparable to foliation S3 from Klepeis (1994; Table 2). The associated F4 folds

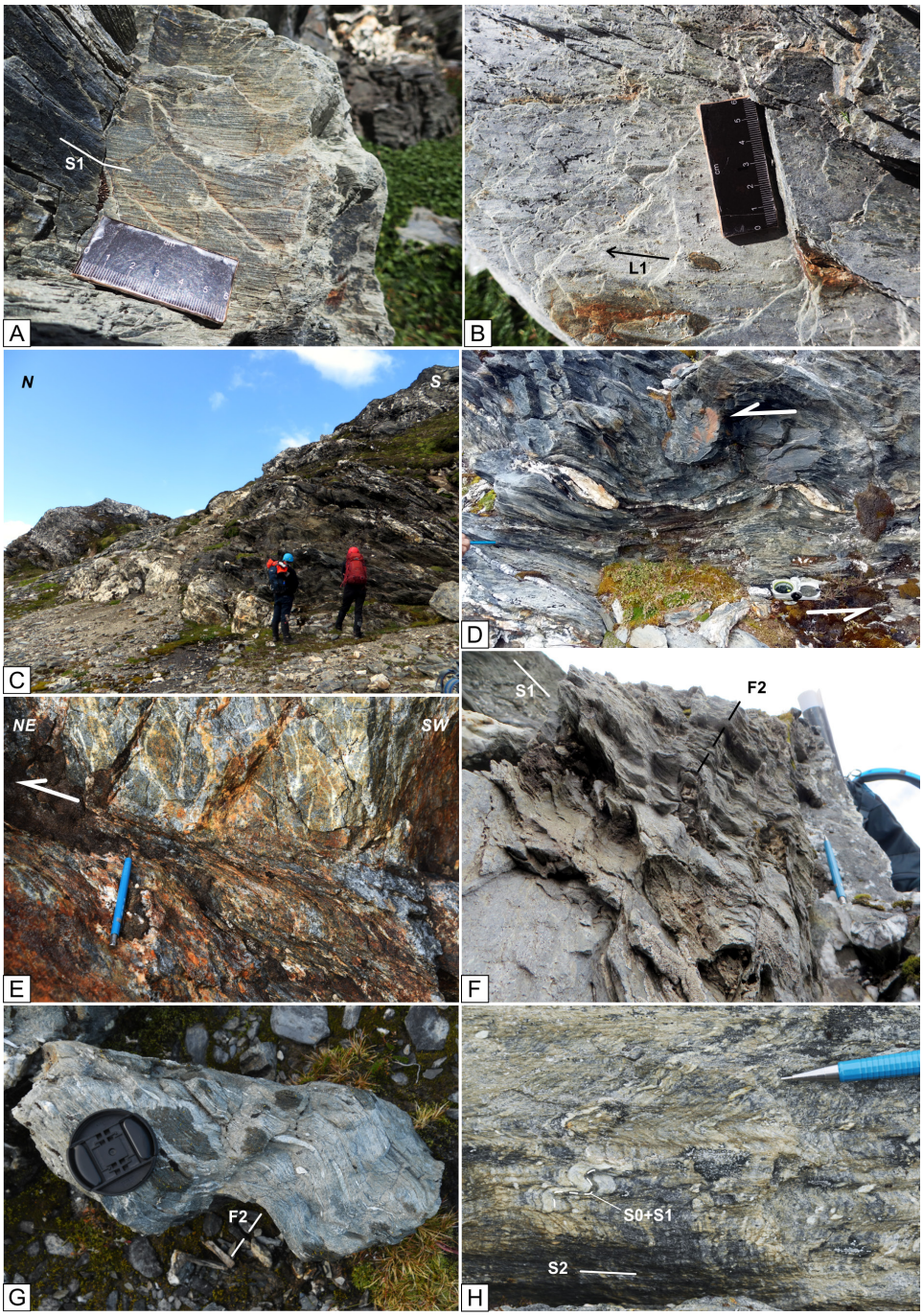

FIG. 4. Structures developed in the footwall of the Glaciar Marinelli Thrust. **A.** S1 foliation in slates intercalated with breccias at point CD01. The transposed stratification remains as dismembered lenses parallel to S1. **B.** L1 stretching lineation in the slates of A, defined by stretched porphyroclasts. **C.** Outcrop example of a brittle-ductile shear zone at CD02. **D.** Detail of the same zone, with deflected S1 surfaces revealing a top-to-northeast shear sense. **E.** Similar fabric at point CD10, where a shear band separates more distributed (ductile) deformation (bottom) from a brittle breccia (top). **F-G.** F2 folds developed on S1 surfaces between points CD04 and CD05 (F), and on breccias near point CD06 (G). Dashed lines indicate F2 axial traces. **H.** Macroscopic relationship between the S2 crenulation cleavage that cross-cuts the transposition foliation formed by parallel S0+S1, in a fine breccia at point CD04.

described by this author are the crenulation folds and sigmoidal deflections formed near shear bands in brittle-ductile thrust zones, which we label F2. The intersection of S2 with S1 surfaces forms a crenulation lineation (L2), which is subparallel to F2. We did not recognize the fine-spaced cleavage at low angle to S1 briefly mentioned by Klepeis (1994), which he labels S2. Accordingly, our S2 foliation corresponds to the S2 foliation of northern Cordillera Darwin (Nelson *et al.*, 1980; Table 2).

4.1.2. Hanging wall of the Glaciar Marinelli Thrust

The Glaciar Marinelli Thrust manifests as a brittle-ductile fault zone characterized by brecciated rock, with profuse quartz veins. The outcrop width is at least 10 to 20 m, partly covered by debris, and distinguished in the field as a prominent escarpment in the western flank of the Cañadón del Horno headwaters (Fig. 5A, B). The escarpment has a WNW-ESE trend (Fig. 2). The fault affects fine phyllites and breccias, the latter similar to those described in the footwall. Profuse shear bands with sigmoidal deflection in the dominant foliation (see below) indicate a top-to-north/northeast shear sense, as reported by Klepeis (1994; Fig. 5C, D). Discrete brittle faults cut the previous foliations within the brittle-ductile fault zone.

For at least one kilometre (between CD05 and CD25), the hanging wall of the fault is composed of the same metasedimentary phyllites and fine schists. These rocks reveal a finely spaced foliation, more or less micaceous, which clearly affected the original sedimentary layering (S0). The sedimentary layering is folded into isoclinal folds (F1) and is mostly transposed by the dominant foliation, which is the same S1 foliation that was described in the footwall (Fig. 5E-H). The microlithons of S1, therefore, comprise rootless F1 folds and discontinuous S0 bands (Fig. 5E). The S1 foliation is also affected by the S2 crenulation foliation and F2 folds, which are very well developed near brittle-ductile thrust faults (Fig. 5D), as observed at CD25 and CD05. In general, the studied transect in the hanging wall of the Glaciar Marinelli Thrust reveals a more profuse development of S2 than the footwall. In some exposures, the S2 foliation is variably developed at outcrop scale, showing horizons where it completely transposes S1, and others of equivalent thickness where it becomes more widely spaced (Fig. 6A-C).

The sedimentary layering in the phyllites is formed by alternating stripes of lighter quartz-rich material and darker very fine material, which is recognized in the microlithons of the S1 transposition foliation, especially in the hinges of rootless F1 folds (Fig. 5E, G). Under the microscope, the lighter bands are composed of fine metapsammite horizons, with grains smaller than 200 μm and in general smaller than 50 μm of quartz and feldspar (mostly plagioclase; Figs. 5F-H and 6D-H). Quartz reveals grain size reduction due to dynamic recrystallization by subgrain rotation, which results in new individuals of 20 to 30 μm, with polygonal grain boundaries. Some of these polygonal boundaries appear affected by subsequent bulging recrystallization that modifies them into lobulated boundaries.

These metasedimentary rocks are cut by coarse quartz veins, which show both oblique and subparallel boundaries with the metapsammites, although the original contacts are highly deformed and partially recrystallized (Figs. 5G-H and 6G-H). The quartz in the veins has sizes up to 0.5-0.6 mm, with polygonal or rectilinear grain boundaries affected by later bulging (as mentioned for the metapsammites), and reveals undulose extinction and subgrain formation. Acicular muscovite within the quartz crystals produces pinning structures in some grain boundaries. Occasional chlorite fibres are included in these quartz veins.

Both the metapsammite and the quartz veins are intercalated with bands of metapelite, in which the fine protolith is replaced by metamorphic euhedral muscovite with preferred orientation, less dominant chlorite (also euhedral in fibres or aggregates), and euhedral biotite porphyroblasts (Figs. 5F-H and 6F-H). Alteration in the biotite produces a faint coloration and, in some cases, it is replaced by pseudomorphic chlorite. Accessory minerals include many detrital zircon grains.

In agreement with the macroscopic observations, the microstructure reveals rootless isoclinal F1 folds in the banded metapsammite-metapelite horizons denoting the original stratification (S0), as well as in the quartz veins (Fig. 5F-H). The S1 transposition foliation is well developed, parallel to F1 axial traces, and defined by the orientated metamorphic muscovite, chlorite, and biotite, and pressure-solution seams. These metamorphic minerals thus formed coevally with development of S1 and F1, together with the granoblastic texture of the veins and the polygonal grains of the metapsammite bands. The latter are clearly

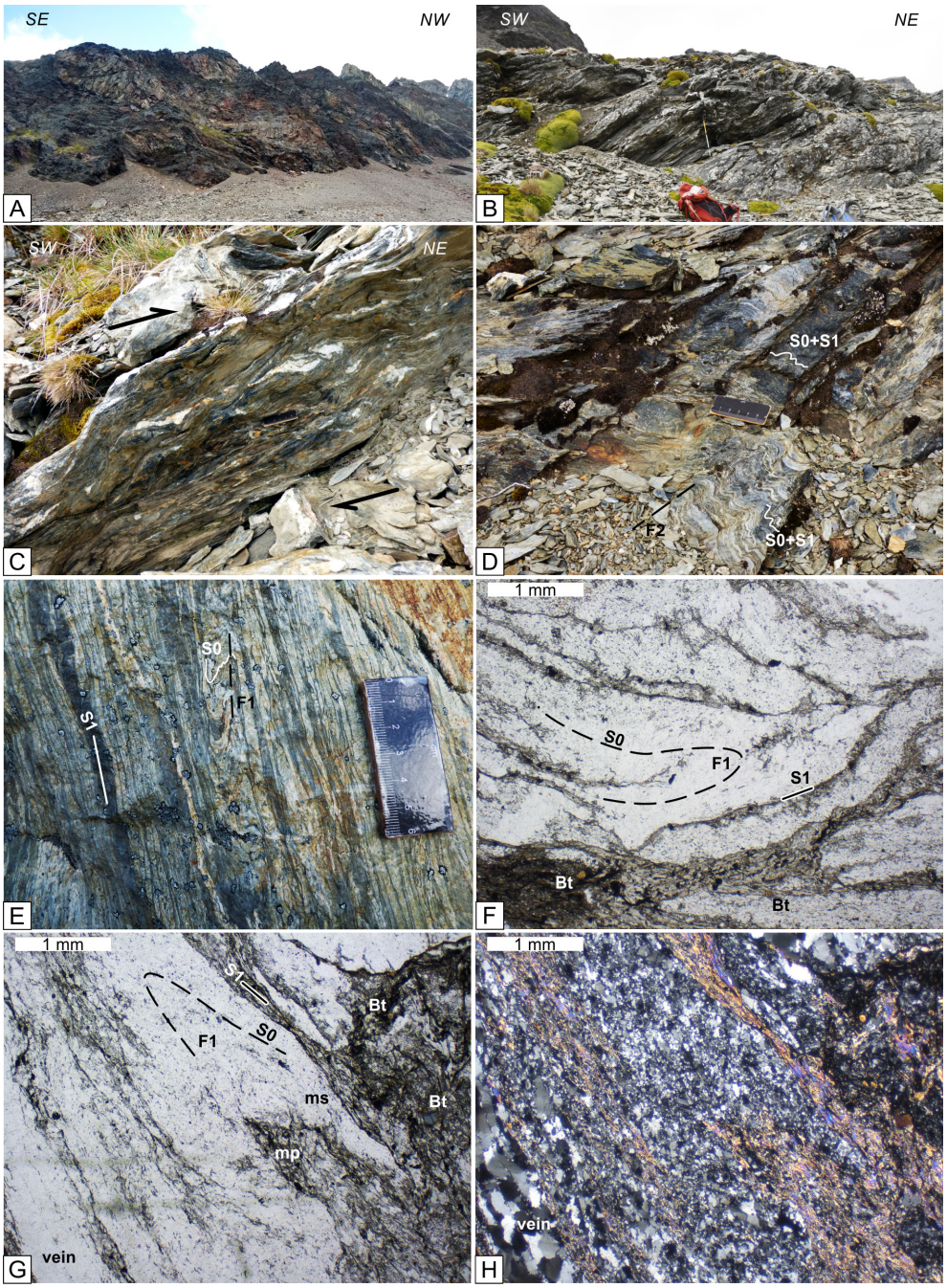

FIG. 5. **A.** Outcrop of the Glaciar Marinelli Thrust at point CD05. The basal part of the cliff, partly covered by debris, is a 20-30 m thick fault zone. **B.** Outcrop of the fault zone, from the left end of the escarpment shown in A. **C-D.** Detail of the brittle-ductile fabric, revealing sigmoidal deflection (C) and F2 folds (D) in the transposed sedimentary layering (S0+S1). Photographs from the fault zone shown in B. **E.** Macroscopic view of rootless, isoclinal F1 folds in S0 laminae, and discontinuous S0 bands preserved within the S1 transposition foliation. The dashed black line marks the axial trace of a F1 fold, parallel to S1. Photograph from the footwall directly below the Glaciar Marinelli Thrust. **F-H.** Photomicrographs showing the relationships between S0, the S1 transposition foliation, subparallel veins, and isoclinal F1 folds. mp: metapelite, ms: metapsammite. Notice biotite porphyroblasts (Bt) in the fine micaceous laminae. Detailed descriptions in text. F-G: plane-polarized light, H: same photo as G, cross-polarized light.

affected by subsequent lower grade deformation and dynamic recrystallization, reflected by the deformed quartz with lobulated boundaries that obliterate the prior rectilinear boundaries.

A zoned S2 crenulation foliation deforms both the F1 folds and S1 foliation, forming F2 folds (Fig. 6D-H). A sample from CD23 clearly illustrates the relationship between F2/S2 and the prior fabrics. We cut two thin sections from this sample, one from the hinge zone of an F2 fold (Fig. 6D), and the second from the "long" back-limb of the same fold (Fig. 6E). In Fig. 6E a clear subparallel relationship between S0 and S1 is observed, as well as the metasedimentary texture of the protolith. The S1 foliation has smooth cleavage domains 0.1-0.2 mm thick, preferentially formed in the transposed metapelitic protolith, that separate 1.4-0.4 mm thick microlithons. The latter are formed by bands of metapsammite, with fine sand-silt grains of quartz and feldspar, large detrital muscovite grains, and a completely orientated fabric. The microlithons have less abundant fine muscovite-sericite, chlorite and biotite. Discontinuous pressure-solution seams in the microlithons are parallel to the S1 foliation. In this long limb of F2, S2 develops as a zonal crenulation, spaced 0.08-0.3 mm at a low angle with respect to S1 (~25°). It has minor, new orientated sericite and occasional biotite, both very fine, in the cleavage domains.

Metapsammitic layers within microlithons of S1 form the thin section cut from the hinge zone of the F2 fold (Fig. 6D). They have variable thicknesses between 40 and 240 μm, being thicker in the hinges of F2 microfolds, and with the same mineralogical characteristics described for figure 6E, including oversized detrital muscovite obliquely orientated compared to metamorphic muscovite-sericite. In this sample, S2 is a well-developed discrete foliation, crosscutting S1 in the limbs of the F2 microfolds (Fig. 6E). The S2 cleavage domains have a variable spacing depending on the size of the clasts, which can be as small as 10-30 μm. They reveal new sericite in a smooth to anastomosed foliation, abundant pressure-solution seams, and some grain-shape preferred orientation of quartz in the hinges of the F2 microfolds. In the microlithons, there is a strong to moderate orientation of the components.

It is necessary to compare these structures with those described by Klepeis (1994) in the hanging wall of the Glaciar Marinelli Thrust (see Table 2 and section 2.3). The "early" S1 foliation described by this author is a combination of the original metapelitic-metapsammitic layering and quartz veins that we describe above (S0), and the subparallel or transposition foliation (S1). Accordingly, the isoclinal folds called F2 by Klepeis (1994) are the F1 folds that we recognized in the S0 and the quartz veins (Fig. 5E-H). The "dominant" S2 foliation described by Klepeis (1994) as a crenulation cleavage overprinting his S1 and axial-planar to his F2, is coplanar with the S1 foliation recognized in the footwall of the Glaciar Marinelli Thrust. This "dominant" foliation is thus parallel to our isoclinal F1 folds, and is therefore the S1 transposition foliation that we observe in the field and describe in our thin sections (Fig. 5E-H): it is the same S1 foliation present in the footwall of the thrust. Accordingly, the S3 crenulation of Klepeis (1994) corresponds to our S2, which is associated with folding (his F3, equal to our F2; Fig. 6). According to Klepeis (1994), shear bands with top-to-northeast shear sense (F4 in his work) bend these folds and crenulation. These are the same shear bands described here, associated with the F2 folds and deflected S1 in the brittle-ductile shear zones (Fig. 5C, D).

In summary, the same structural generations recognized in the footwall are present in the hanging wall. The key to defining this structural sequence is the recognition of the transposed metasedimentary bands as the primary S0 of the protolith.

4.2. Geochronological results

4.2.1. Sample CD05, metasedimentary phyllite from the hanging wall

Unfortunately, very few zircon grains could be retrieved from sample CD05: 45 were analysed (Supplementary File 2). They were imaged by cathodoluminescence images (Supplementary File 5) and show different sizes and shapes, from sub-euhedral to sub-rounded. The grains yield variable U and Pb contents (81-3155 ppm and 58-4711 ppm, respectively), Th/U ratios (0.03 to 0.6), as well as apparent ages (447 to 1886 Ma). In a KDE diagram (Fig. 7A), the ages define three main peaks: around 1000, 770, and 530 Ma. These zircon grains are detrital in origin, with a few (n=5) yielding metamorphic Th/U ratios below 0.1 (apparent ages of 1886±12, 1202±24, 973±42, 625±23, and 447±20 Ma), while most have Th/U ratios compatible with a magmatic

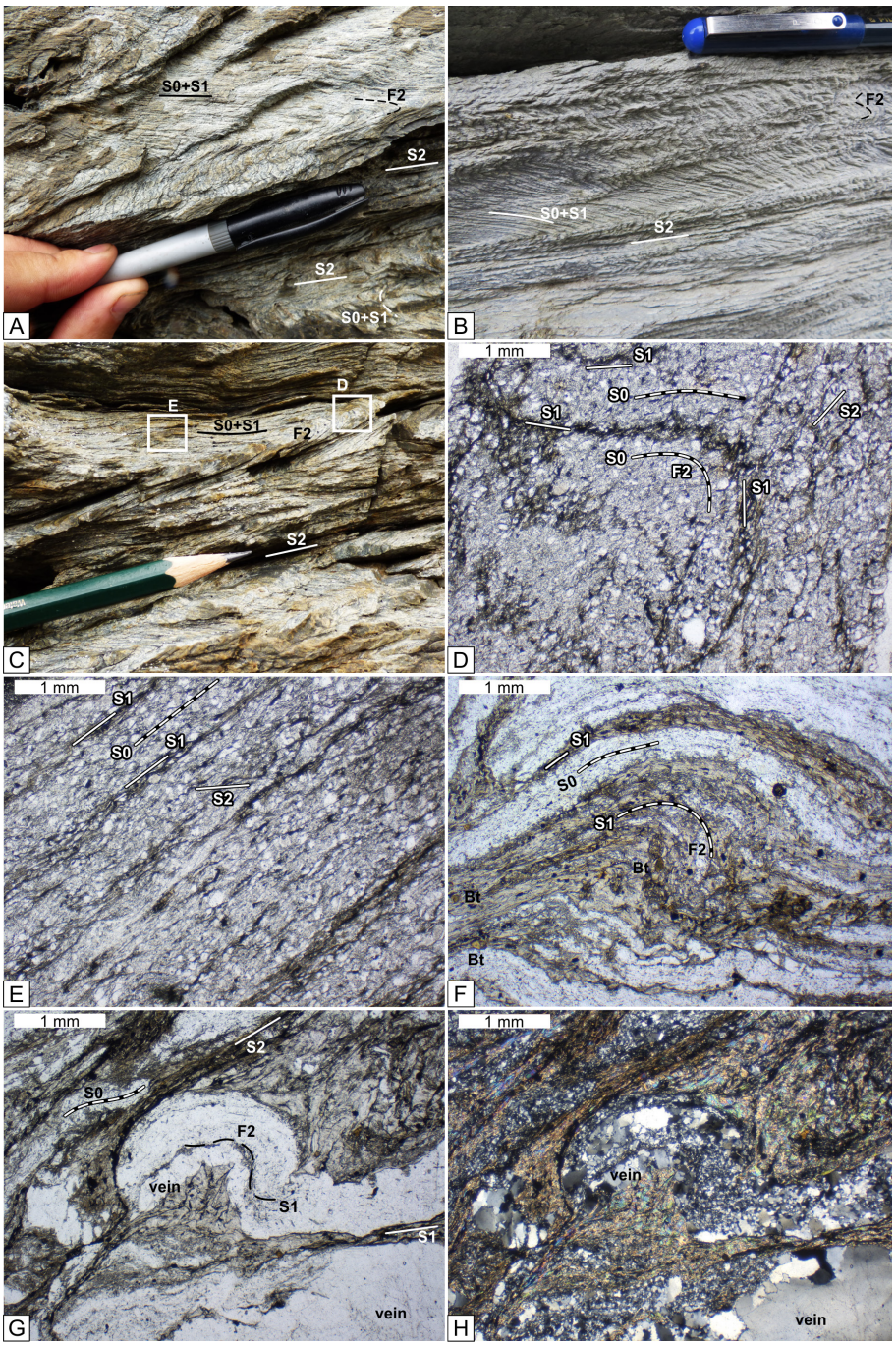

FIG. 6. **A-B.** Folded S0+S1 bands (S1 transposition foliation with discontinuous subparallel S0 in the microlithons) forming F2 asymmetric folds, axial planar to the S2 crenulation cleavage in the fine schists and phyllites of the Glaciar Marinelli Thrust hanging wall. Notice stronger development of the S2 cleavage at some horizons, where it transposes all prior fabrics into a closely spaced crenulation cleavage. **C.** Similar structure showing equivalent location of photomicrographs D and E (sample CD23), in the hinge zone and limb of an F2 fold. **D-E.** Photomicrographs revealing the relationships between the F2-S2 fabric on prior transposition foliation (S1) and subparallel S0 bands, with better development of S2 in the hinge zones. **F-H.** Photomicrographs revealing folded transposition foliation subparallel to quartz veins, forming F2 folds with axial-planar S2 crenulation cleavage. D-G: plane-polarized light, H: cross-polarized light, same photo as G.

origin (Th/U>0.1). For this sample the YSG and Y3Go ages are Ordovician, 447±20 Ma and 471±12 Ma, respectively (Fig. 7A; Supplementary File 2), while the MLA is less precise and within error of these calculations at 454±28 Ma.

4.2.2. Sample CD06, metapsammite from the footwall

Sample CD06 provided numerous zircon grains, from which we analysed 111 (Supplementary File 2). As for sample CD05, the cathodoluminescence images (Supplementary File 6) display various shapes and sizes for the zircon grains, from euhedral to rounded. They have variable U and Pb contents (21 to 2589 ppm and 20 to 4187 ppm, respectively), as well as Th/U ratios (0.01 to 1.12), suggesting that nine grains have a metamorphic origin with ages of *ca.* 1270, 800-770, 640-600, and 580-520 Ma. The remaining grains yield magmatic signatures. These observations indicate that the zircon grains were derived from different rock types, underscoring their detrital origin. They yielded apparent ages from 309 Ma to 3535 Ma. The KDE diagram shows several age peaks, the three main ones at 610, 520, and 400 Ma (Fig. 7B). For this sample, the YSG age is 309±9 Ma (late Carboniferous) while the Y3Go age is 336±5 Ma (early Carboniferous) (Fig. 7B; Supplementary File 2). The MLA is intermediate at 314±11 Ma.

5. Discussion

5.1. Structural generations and deformation sequence in the study area

Table 2 shows the correlation between the structures previously described in our study area, and those recognized in our work. As can be noticed, we identified the same generations of structures as Klepeis (1994; S1 and S2-F2) in the footwall of the Glaciar Marinelli Thrust, except for a "fine spaced cleavage at low angle to S1". We do not know the meaning of this later fabric, which is not clearly described by the mentioned author and we did not recognize it in the field or in thin section. In the hanging wall of the thrust, we noticed the same generations as in the footwall. However, according to Klepeis (1994) there is an additional and older tectonic fabric (S1 in his work), which he considered part of the pre-Andean Db deformation of Nelson *et al.* (1980; Table 2). As established in section 4.1, this early fabric has been confused with the transposed S0, which is dismembered and isoclinally folded, forming discontinuous bands subparallel to the main transposition S1 (Fig. 5E-H). This confusion could have influenced the assignment of the hanging wall rocks to the basement units in previous work. Therefore, it is critical to determine the precise generation of structures in that area.

Our work shows that the same structural events affected the hanging wall and footwall of the Glaciar Marinelli Thrust. The sequence of deformation comprises a first ductile deformation producing the main cleavage (S1), which varies from a spaced cleavage in more competent rocks (rhyolites, metapsammites) and a transposition cleavage in phyllites and slates (Fig. 8A, B). The transposition cleavage is clearly manifested in the more deformed rocks of the hanging wall, where the original sedimentary lamination (S0) remains as rootless isoclinal folds between cleavage domains (Fig. 5E-H). This deformation was coeval with, or slightly preceded, the higher metamorphic grade revealed by euhedral biotite porphyroblasts (Figs. 5F-H and 6F-H). The subsequent deformation resulted in brittle-ductile thrusts such as the Glaciar Marinelli Thrust (Fig. 8C). These shear zones were accompanied by folding and crenulation of the prior S1 fabrics forming the S2 crenulation foliation, F2 folds, and related structures (Figs. 4D-H, 5C-D, and 6). This deformation occurred without significant metamorphism.

These two structural generations reflect the known history of deformation elsewhere in the Fuegian Andes: a ductile contractional deformation, associated with the closure of the Rocas Verdes Basin ($D1_{CB}$), and the subsequent development of the Fuegian thrust-fold belt ($D2_{CB}$), as mentioned in section 2.1 (Fig. 8). The rocks studied in this work show no deformation prior to $D1_{CB}$ structures, suggesting either that 1) these rocks are Paleozoic basement without pre-Jurassic deformation, or that 2) they comprise part of the sedimentary and volcanic deposits of the Rocas Verdes Basin. We consider that the first possibility is highly improbable, since it would imply that these rocks covering the Upper Devonian Svea granite remained without any trace of penetrative deformation until the Late Cretaceous closure of the Rocas Verdes Basin. In other words, they would have persisted *ca.* 260 Myr in the SW margin of Gondwana unaffected by the proposed late Paleozoic-early Mesozoic episodes of regional deformation in that margin (*e.g.,* Ramos, 2008;

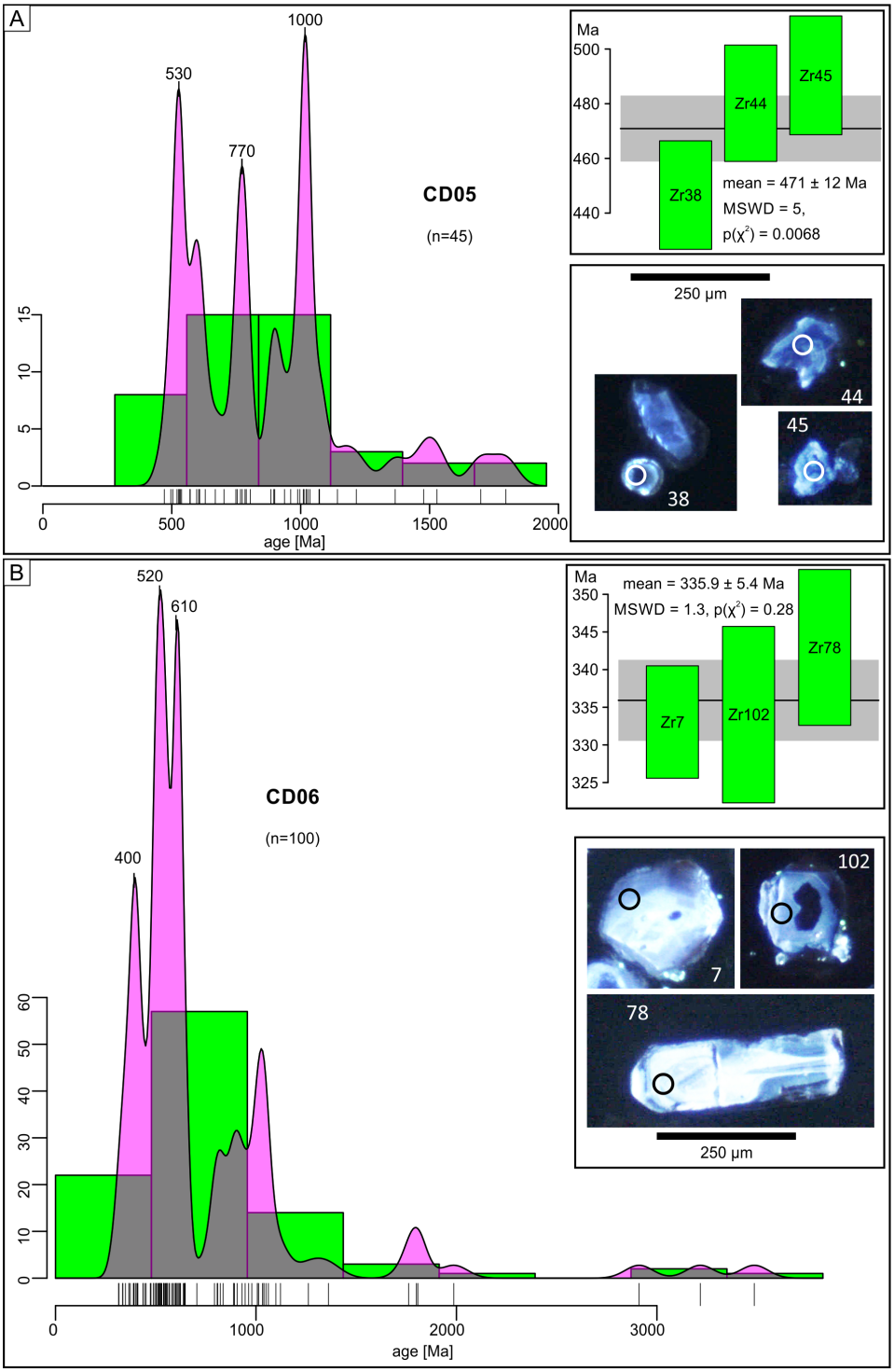

FIG. 7. Geochronological results of samples CD05 (A) and CD06 (B). KDE diagrams show main Cambrian and Proterozoic peaks. Insets display the Y3Go ages for each sample, with labels indicating the grains used (bar heights are ±2σ). Cathodoluminescence (CL) images of the grains used in the Y3Go age calculations are shown for each sample (see complete CL images in Supplementary Files 5 and 6), notice variable roundness and broken grains. MSWD: mean standard weighted deviation.

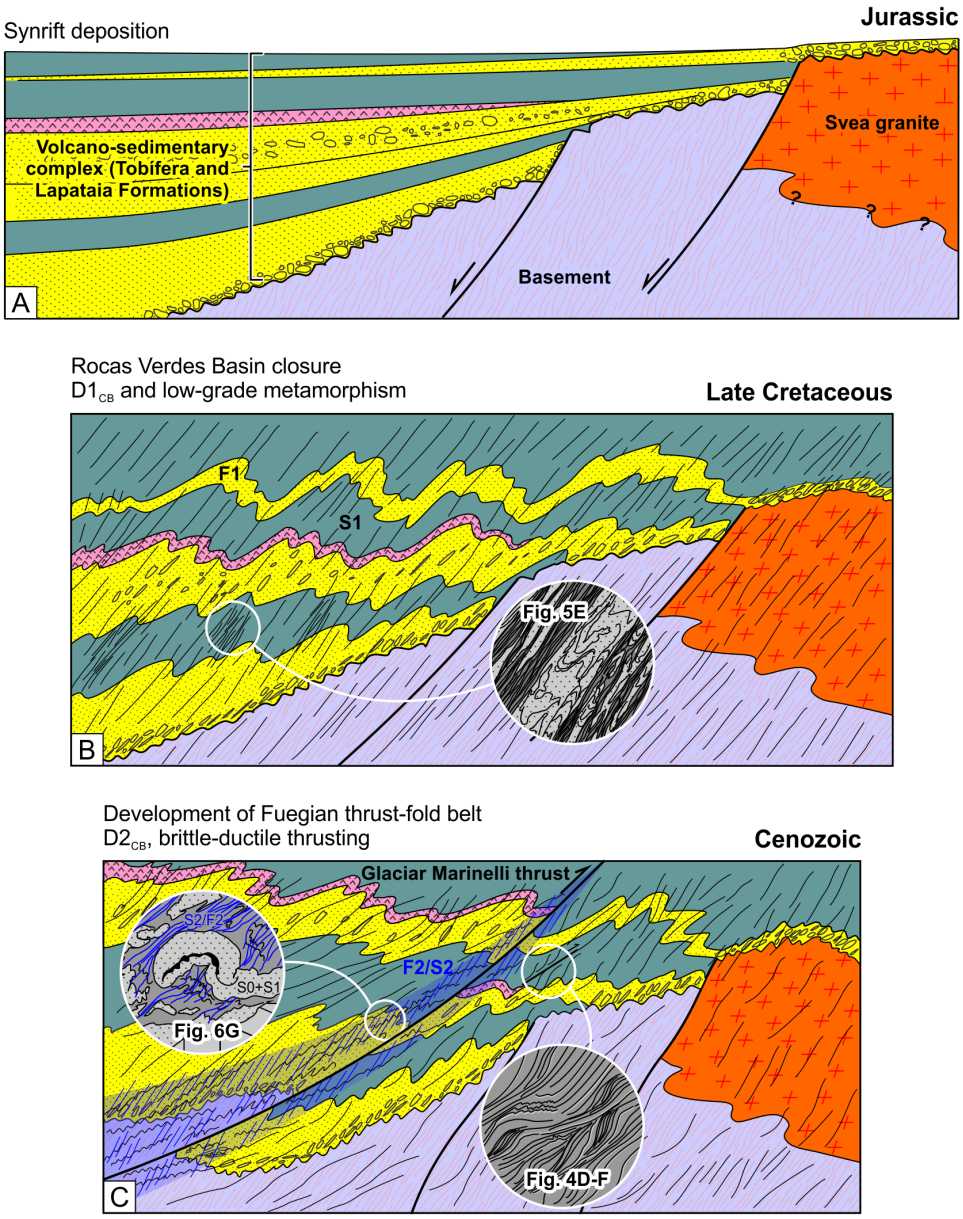

FIG. 8. Cartoon depicting the deformation sequence interpreted from our structural and petrographic data, in the context of the tectonic evolution of the Fuegian Andes. **A.** Jurassic. **B.** Late Cretaceous. **C.** Cenozoic. The extent and cross-cutting relationships of the Svea granite and the normal fault drawn in A, as well as the geometry of the hemigraben, are theoretical and not to scale.

Castillo *et al.*, 2017; Riley *et al.*, 2023). This is very unlikely, and local basement rocks are indeed deformed by pre-Jurassic penetrative structures (Nelson *et al.*, 1980; Klepeis *et al.*, 2010; Hervé *et al.*, 2010a). We conclude that the studied rocks form part of the Rocas Verdes Basin cover.

5.2. Stratigraphy of the footwall and hanging wall rocks of the Glaciar Marinelli Thrust

The problem of distinguishing between cover rocks and basement in Cordillera Darwin is an issue documented since early geological work in the area

(Kranck, 1932; Fester, 1938). This is especially so for fine-grained metasedimentary rocks, since coarser rocks in the cover may bear foliated clasts interpreted as eroded basement. For example, despite Kranck (1932) repeatedly describing "old basement schists" or "high metamorphic schists" as dominantly quartz-micaceous fine schists, he also recorded these facies intermingled with the Tobífera Formation in the fjords of northern Cordillera Darwin and with coarser facies in the Lapataia Formation (see section 2.2.1). Subsequent work included some of these fine schists either within the basement or within the cover rocks, as we can observe comparing maps and sample descriptions from Nelson *et al.* (1980), Johnson (1990), and Ortiz (2007).

The usage of geochronological dating, especially U-Pb dating in zircons, has provided valuable information on the nature and origin of the rocks in this region. However, sediments deposited above the basement without particularly profuse synchronous volcanism (*e.g.*, in a synrift environment), are likely to reflect zircon ages of the eroded basement instead of syndepositional ages (Cawood *et al.*, 2012; Copeland, 2020; Castillo *et al.*, 2022). This has been reported for the Mesozoic cover rocks of the Fuegian Andes (Hervé *et al.*, 2010a; Cao *et al.*, 2022, 2025), and in similar back-arc or rift settings (Rossignol *et al.*, 2019). In this context, detailed petrographic studies are crucial to complement the geological significance of geochronological determinations.

Hervé *et al.* (2010a) proposed a working hypothesis for distinction between cover and basement within the northern Cordillera Darwin Metamorphic Complex, arguing that samples with Permian or Triassic zircons and without Jurassic zircons can be considered part of the Rocas Verdes Basin, whilst samples with Carboniferous or older ages may be part of the basement. They advised caution regarding this presumption, however, and we indeed consider that it is challenged by the evidence from the Lapataia Formation (see below), but also from rocks within the Cordillera Darwin Metamorphic Complex that bear sparse Jurassic grains, and abundant zircons with ages older than the Permian (Hervé *et al.*, 2010a; see Table 3). All these samples have scarce but sufficient petrographic or geochronological evidence that proves they belong to the Mesozoic cover, having sparse or no late Paleozoic or Triassic zircon grains. Thus, lower Paleozoic rocks have to be considered as important sources for detrital zircons in the Rocas Verdes Basin fill, as can be inferred from the ages of the metamorphic zircons in our dataset. Conversely, to use the lack of Permo-Triassic age signatures in a rock as evidence that this rock belongs to the basement, is disputable.

Petrographic analysis of the rocks studied in this work reveals facies comparable to the Tobífera Formation and Lemaire Complex (*i.e.,* volcanic, volcaniclastic, and sedimentary rocks), and with the Lapataia Formation (metasedimentary and metabasic rocks). The former are distributed in the footwall of the Glaciar Marinelli Thrust, including the Estratos Paso de las Lagunas of Mella and Quiroz (2023), previously mapped as the La Paciencia Formation by Klepeis (1994; Table 1; Supplementary File 1). We consider that the facies shown in figure 4 are significant enough to discard the latter argument, since the La Paciencia Formation is mostly metapelitic according to Cortés and Valenzuela (1960) and later work (see Cañón, 2000).

As defined by Mella and Quiroz (2023), the Estratos Paso de las Lagunas are composed of metasedimentary rocks, including quartzites and metaconglomerates, unconformably covering the Upper Devonian Svea granite and an associated early Carboniferous orthogneiss. Sample CD06 from Paso de las Lagunas is a metapsammite intercalated with breccias that yields a Carboniferous MDA (between *ca.* 339 and 310 Ma, depending on the MDA calculation method used), and a rather continuous record of detrital Paleozoic ages with a marked late Neoproterozoic-Cambrian peak. An older peak contains late Grenvillian Neoproterozoic ages (~0.8-1.0 Ga; Fig. 7B). We consider the facies of sample CD06 to be very closely similar to that of the Lemaire Complex and Tobífera Formation along the northern flank of Cordillera Darwin and in Argentina (Johnson, 1990; Olivero and Martinioni, 1996; Ortiz, 2007; Hervé *et al.*, 2010a). This interpretation is made notwithstanding the Paleozoic detrital zircon ages and is consistent with similar interpretations elsewhere in the region. Notice for example the metasandstone of sample FO0524 described by Ortiz (2007), with foliated metamorphic rock fragments comprising 25% of the sample, and dated by Hervé *et al.* (2010a; see Table 3). Despite its Triassic MDA and prominent Cambrian age peak, and the lack of Jurassic ages, this rock is very likely part of the sedimentary fill of the Rocas Verdes Basin.

TABLE 3. SUMMARY OF SAMPLES FROM NORTHERN CORDILLERA DARWIN DATED BY HERVÉ *ET AL.* (2010a) AND DISCUSSED IN THIS WORK.

Sample	Lithology	Unit (sensu Hervé *et al.*, 2010a)	Zircon U-Pb ages
FO0539	Foliated quartzose phyllite from a conglomeratic succession that conformably underlies an ignimbrite bed.	Tobífera Formation (Basal Clastic Complex)	Dominant Carboniferous peaks (*ca*. 340-360 Ma), and older peaks and scattered ages. Two grains record Jurassic dates (3 spots, one from SHRIMP).
FO0508	Quartz-rich amphibole-bearing foliated rock.	Cordillera Darwin Metamorphic Complex (interpreted Tobífera Formation Basal Clastic Complex)	Dominated by Early Devonian peak (404±5 Ma). Pre-Devonian ages between 600-680 Ma. 9 spots in 6 grains of Jurassic age, eight form a peak around 166±2 Ma. These ages come from grains that are predominantly igneous in origin.
FO0516	Granitic clast from a matrix-supported foliated conglomerate.	Tobífera Formation (Basal Clastic Complex)	Single population of zoned igneous zircon, 18 grains give a weighted mean age of 466±3 Ma (Ordovician).
FO0524	Feldspathic litharenite, with quartz, plagioclase, slate or phyllite, quartzite and marble clasts. Foliated metamorphic rock fragments comprise 25% of the sample (Ortiz, 2007). It is part of a succession in which clast-supported conglomerates containing 1-10 cm pebbles of quartz, micaschist and volcanic rocks predominate.	Tobífera Formation (Basal Clastic Complex)	Predominant broad Cambrian peak (*ca.* 530-550 Ma). Youngest peaks of Permian and Triassic ages at *ca.* 270 and 245 Ma. Scattered older ages.

Sample CD06 also reveals clasts of metamorphic rocks, alike other sandstones and breccias cropping out in the footwall of the Glaciar Marinelli Thrust (Fig. 3E, F, H), a feature that has been also recognized in the Lapataia Formation and in the Lemaire Complex (Cao *et al.*, 2022, 2025). The Lemaire Complex sandstones exposed in the footwall of the Mina Beatriz thrust (Fig. 1), for example, described by Olivero and Martinioni (1996), reveal clasts of foliated rocks and are interlayered with tuffs and rhyolites. In a similar way, the interlayered metatuffs and rhyolite in the metasedimentary succession of Paso de las Lagunas suggests the assignment of these rock exposures to the Tobífera Formation (Fig. 2). This leaves the explanation of the Paleozoic U-Pb detrital zircon ages of sample CD06 as a signature derived from the prominent supply of detritus from eroded basement rocks, probably influenced by the nearby Svea granite, as shown schematically in figure 8A.

Likewise, the phyllites of the hanging wall of the Glaciar Marinelli Thrust are composed of facies that resemble the phyllites and schists of the Lapataia Formation in Argentina. The latter is well known in the hanging wall of the Mina Beatriz thrust, which has been traced regionally and correlated with the Glaciar Marinelli Thrust (Cao *et al.*, 2022, 2023; Fig. 1). Previous work in our study area assigned the rocks in the hanging wall of the Glaciar Marinelli Thrust to the basement (Klepeis, 1994; Supplementary File 1) or to the Cordillera Darwin Metamorphic Complex (Rojas and Mpodozis, 2006; Hervé *et al.*, 2010a). Similarly, the Lapataia Formation has been considered part of the Paleozoic basement of the Fuegian Andes for many years (Kranck, 1932; Borrello, 1972; Bruhn, 1979). However, recent work established its inclusion in the Mesozoic cover based on the absence of a pre-Andean foliation and the occurrence of deformed, foliated, inherited rock fragments within the Formation (Cao *et al.*, 2018, 2022). The strata cropping out in the hanging wall of the Glaciar Marinelli Thrust show the same petrographic and microstructural characteristics, as

mentioned in previous sections. Regardless of the calculation method used for the MDA, sample CD05 from the hanging wall rocks yields an Ordovician MDA, and older clusters of latest Neoproterozoic-early Cambrian and ~1.1-0.8 Ga age groups that are comparable to those observed in sample CD06 (Fig. 7). These age clusters are also comparable to the ages found in the Lapataia Formation (Cao *et al.*, 2022), consistent with the provenance from an eroded Paleozoic basement during the early development of the Mesozoic syn-rift deposits in the absence of coeval volcanism (Fig. 8A). The lack of younger Paleozoic zircons, compared with sample CD06, reveals different source areas within the Jurassic basin and probably different structural levels, prior to reverse faulting along the Glaciar Marinelli Thrust.

Neoproterozoic-Cambrian and Grenvillian zircons are largely documented in basement rocks and in the detrital record of the Mesozoic cover of the Fuegian Andes (*e.g.*, Hervé *et al.*, 2010a). Recent paleogeographic reconstructions of Gondwana assembly propose a Neoproterozoic-Cambrian arc on the paleo-Pacific margin of the East Antarctica craton, which was located adjacent to the north Patagonian and south Patagonian (Magallanes Basin basement) blocks (González *et al.*, 2018). Older zircons, derived from eroded Grenvillian mobile belts, are expectedly abundant in the basement of these blocks.

6. Conclusions

Detailed petrographic and structural observations in the hanging wall of the Glaciar Marinelli Thrust reveal Late Cretaceous-Cenozoic ductile ($D1_{CB}$) and brittle-ductile ($D2_{CB}$) structures, associated with the closure of the Rocas Verdes Basin and later development of the Fuegian thrust-fold belt. No older structures were recognized, and previous interpretations of a "pre-Jurassic" deformation in these rocks were probably influenced by the difficult recognition of the transposition of the original sedimentary layering by the Late Cretaceous $D1_{CB}$ (S1) main foliation. We identify the same structure generations in the metasedimentary-metavolcanic sequence exposed in the footwall of the Glaciar Marinelli Thrust.

These structural relationships, as well as the facies of the rocks in our study area, indicate that these are metasedimentary rocks of the Rocas Verdes Basin cover. Accordingly, the footwall rocks reveal protolith facies identical to those recognized in the Tobífera Formation-Lemaire Complex (Middle Jurassic-Berriasian), which include rhyolite, breccias, sandstones and finer facies (tuffs and pelite). In the hanging wall, breccias and fine metasedimentary rocks with a higher degree of deformation resemble the facies recognized in the Jurassic Lapataia Formation. The detrital zircons obtained from two samples in these units have Ordovician and Carboniferous youngest U-Pb ages, and several older age peaks, indicative of a sediment source in basement highs exposed during syn-rift deposition. The Upper Devonian Svea Granite is an excellent example of such basement exposures in our study area. This work emphasizes the need for detailed petrographic and structural analyses to complement geochronological studies, when aiming to make stratigraphic determinations in rocks with relatively scarce synsedimentary volcanism.

Acknowledgements

This research was funded by ANID through Project Fondecyt 1231211 to FP. We thank CONAF and Cuerpo Militar del Trabajo (CMT) for sampling permission at Yendegaia National Park, Sra. Ivette from Caleta María for logistic support and Sr. César for his hospitality. We also want to thank V. Mosqueira González for help during fieldwork and for granting usage of some of the photographs. Thin sections were prepared by L. Remón (CADIC-CONICET). We thank D. Barbeau, V. Muller, guest editor R. Pankhurst, and editor D. Bertin for their constructive reviews.

References

Álvarez-Marrón, J.; McClay, K.; Harambour, S.; Rojas, L.; Skarmeta, J. 1993. Geometry and evolution of the frontal part of the Magallanes foreland thrust and fold belt (Vicuña Area), Tierra del Fuego, Southern Chile. AAPG Bulletin 77 (11): 1904-1921. https://doi.org/10.1306/BDFF8F74-1718-11D7-8645000102C1865D

Betka, P.; Klepeis, K.; Mosher, S. 2015. Along-strike variation in crustal shortening and kinematic evolution of the base of a retroarc fold-and-thrust belt: Magallanes, Chile 53° S-54° S. Geological Society of America, Bulletin 127 (7-8): 1108-1134. https://doi.org/10.1130/B31130.1

Betka, P.; Mosher, S.; Klepeis, K. 2022. Progressive Development of a Distributed Ductile Shear Zone beneath the Patagonian Retroarc Fold-Thrust Belt, Chile. Lithosphere (1): 3820115. https://doi.org/10.2113/2022/3820115

Borrello, A. 1972. Cordillera Fueguina. *In* Geología Regional Argentina (Leanza, A.F.; editor). Academia Nacional de Ciencias: 741-754. Córdoba.

Bruhn, R.L. 1979. Rock structures formed during back-arc basin deformation in the Andes of Tierra del Fuego. Geological Society of America Bulletin 90 (11): 998-1012. https://doi.org/10.1130/0016-7606(1979)90%3C998:RSFDBB%3E2.0.CO;2

Bruhn, R.L.; Stern, C.R.; De Wit, M.J. 1978. Field and geochemical data bearing on the development of a Mesozoic volcano-tectonic rift zone and back-arc basin in southernmost South America. Earth and Planetary Science Letters 41 (1): 32-46. https://doi.org/10.1016/0012-821X(78)90039-0

Calderón, M.; Fildani, A.; Hervé, F.; Fanning, C.M.; Weislogel, A.; Cordani, U. 2007. Late Jurassic bimodal magmatism in the northern sea-floor remnant of the Rocas Verdes basin, southern Patagonian Andes. Journal of the Geological Society 164: 1011-1022. London. https://doi.org/10.1144/0016-76492006-102

Cañón, A. 2000. Nuevos antecedentes en la estratigrafía de la Cuenca de Magallanes. Anales Instituto de la Patagonia 28: 41-50.

Cao, S.J.; Torres Carbonell, P.J.; Dimieri, L.V. 2018. Structural and petrographic constraints on the stratigraphy of the Lapataia Formation, with implications for the tectonic evolution of the Fuegian Andes. Journal of South American Earth Sciences 84: 223-241. https://doi.org/10.1016/j.jsames.2018.04.002

Cao, S.J.; Torres Carbonell, P.J.; Bordese, S.; Lovecchio, J.P. 2022. Early rifting during marginal basin development: Petrography, microstructure, and detrital zircon U-Pb geochronology of the Lapataia Formation, Argentine Fuegian Andes. Basin Research 34 (4): 1400-1420. https://doi.org/10.1111/bre.12664

Cao, S.J.; Torres Carbonell, P.J.; Sánchez, N.P.; Bordese, S.; Dimieri, L.V. 2023. Thrust tectonics in the Fuegian Andes central belt: A detailed geometric-kinematic analysis and new thermochronological constraints. Tectonophysics 862: 229966. https://doi.org/10.1016/j.tecto.2023.229966

Cao, S.J.; González Guillot, M.; Torres Carbonell, P.J.; Bordese, S.; Lovecchio, J.P.; Dimieri, L.V. 2025. Stratigraphy of the Rocas Verdes basin: Petrography and new U-Pb ages from the Argentine Fuegian Andes. Journal of South American Earth Sciences 152: 105315. https://doi.org/10.1016/j.jsames.2024.105315

Castillo, P.; Fanning, C.M.; Pankhurst, R.J.; Hervé, F.; Rapela, C. 2017. Zircon O- and Hf-isotope constraints on the genesis and tectonic significance of Permian magmatism in Patagonia. Journal of the Geological Society 174 (5): 803-816. https://doi.org/10.1144/jgs2016-152

Castillo, P.; Bahlburg, H.; Fernández, R.; Fanning, C.M.; Berndt, J. 2022. The European continental crust through detrital zircons from modern rivers: Testing representativity of detrital zircon U-Pb geochronology. Earth-Science Reviews 232: 104145. https://doi.org/10.1016/j.earscirev.2022.104145

Cawood, P.A.; Hawkesworth, C.J.; Dhuime, B. 2012. Detrital zircon record and tectonic setting. Geology 40 (10): 875-878. https://doi.org/10.1130/G32945.1

Copeland, P. 2020. On the use of geochronology of detrital grains in determining the time of deposition of clastic sedimentary strata. Basin Research 32 (6): 1532-1546. https://publons.com/publon/10.1111/bre.12441

Cortés, R.; Valenzuela, H. 1960. Estudio geológico del área Lago Blanco - Hito XIX - Monte Hope (porción sur-central de Tierra del Fuego). Empresa Nacional del Petróleo: 22 p. Punta Arenas.

Coutts, D.S.; Matthews, W.A.; Hubbard, S.M. 2019. Assessment of widely used methods to derive depositional ages from detrital zircon populations. Geoscience Frontiers 10 (4): 1421-1435. https://doi.org/10.1016/j.gsf.2018.11.002

Cunningham, W.D. 1994. Uplifted ophiolitic rocks on Isla Gordon, southernmost Chile: implications for the closure history of the Rocas Verdes marginal basin and the tectonic evolution of the Beagle Channel region. Journal of South American Earth Sciences 7 (2): 135-147. https://doi.org/10.1016/0895-9811(94)90004-3

Cunningham, W.D. 1995. Orogenesis at the southern tip of the Americas: the structural evolution of the Cordillera Darwin metamorphic complex, southernmost Chile. Tectonophysics 244 (4): 197-229. https://doi.org/10.1016/0040-1951(94)00248-8

Dalziel, I.W.D. 1986. Collision and Cordilleran orogenesis: an Andean perspective. Geological Society, Special Publications 19 (1): 389-404. London. https://doi.org/10.1144/GSL.SP.1986.019.01.22

Dalziel, I.W.D.; Elliot, D.H. 1971. Evolution of the Scotia Arc. Nature 233: 246-252.

Dalziel, I.W.D.; Brown, R.L. 1989. Tectonic denudation of the Darwin metamorphic core complex in the Andes of Tierra del Fuego, southernmost Chile: implications for Cordilleran orogenesis. Geology 17 (8): 699-703. https://doi.org/10.1130/0091-7613(1989)017%3C0699:TDOTDM%3E2.3.CO;2

Dalziel, I.W.D.; De Wit, M.J.; Palmer, K.F. 1974. Fossil marginal basin in the southern Andes. Nature 250: 291-294.

De la Cal, H.G.; Lajoinie, M.F. 2023. Petrografía del Complejo Ígneo y Metamórfico de Tierra del Fuego en el subsuelo de la Cuenca Austral, Argentina. *In* Congreso de Mineralogía, Petrología Ígnea y Metamórfica, y Metalogénesis, No.14, Actas: 302-305. Bahía Blanca.

Dickinson, W.R.; Gehrels, G.E. 2009. Use of U-Pb ages of detrital zircons to infer maximum depositional ages of strata: A test against a Colorado Plateau Mesozoic database. Earth and Planetary Science Letters 288 (1-2): 115-125. https://doi.org/10.1016/j.epsl.2009.09.013

Fester, G. 1938. La Cordillera Darwin. Anales de la Sociedad Científica Argentina 126 (2): 87-88.

González Guillot, M.; Urraza, I.; Acevedo, R.D.; Escayola, M. 2016. Magmatismo básico jurásico-cretácico en los Andes Fueguinos y su relación con la Cuenca Marginal Rocas Verdes. Revista de la Asociacion Geológica Argentina 73 (1): 1-22.

González, P.D.; Sato, A.M.; Naipauer, M.; Varela, R.; Basei, M.; Sato, K.; Llambías, E.J.; Chemale, F.; Dorado, A.C. 2018. Patagonia-Antarctica Early Paleozoic conjugate margins: Cambrian synsedimentary silicic magmatism, U-Pb dating of K-bentonites, and related volcanogenic rocks. Gondwana Research 63: 186-225. https://doi.org/10.1016/j.gr.2018.05.015

Hanson, B.; Wilson, T. 1991. Submarine rhyolitic volcanism in a Jurassic proto-marginal basin, southern Andes, Chile and Argentina. *In* Andean magmatism and its tectonic setting (Harmon, R.; Rapela, C.; editors). Geological Society of America, Special Papers: 13-27. Boulder.

Hervé, F.; Nelson, E.; Kawashita, K.; Suárez, M. 1981. New isotopic ages and the timing of orogenic events in the Cordillera Darwin, southernmost Chilean Andes. Earth and Planetary Science Letters 55 (2): 257-265. https://doi.org/10.1016/0012-821X(81)90105-9

Hervé, F.; Fanning, C.M.; Pankhurst, R.J.; Mpodozis, C.; Klepeis, K.; Calderón, M.; Thomson, S.N. 2010a. Detrital zircon SHRIMP U-Pb age study of the Cordillera Darwin Metamorphic Complex of Tierra del Fuego: sedimentary sources and implications for the evolution of the Pacific margin of Gondwana. Journal of the Geological Society 167 (3): 555-568. https://doi.org/10.1144/0016-76492009-124

Hervé, F.; Calderón, M.; Fanning, C.M.; Kraus, S.; Pankhurst, R.J. 2010b. SHRIMP chronology of the Magallanes Basin basement, Tierra del Fuego: Cambrian plutonism and Permian high-grade metamorphism. Andean Geology 37 (2): 253-275. http://dx.doi.org/10.5027/andgeoV37n2-a01

Johnson, C. 1990. Antecedentes estratigráficos de la ribera Sur del Seno Almirantazgo. Memoria de título (Inédito), Universidad de Chile, Departamento de Geología y Geofísica: 122 p.

Katz, H.R. 1963. Revision of Cretaceous stratigraphy in Patagonian cordillera of Ultima Esperanza, Magallanes Province, Chile. AAPG Bulletin 47 (3): 506-524. https://doi.org/10.1306/BC743A5D-16BE-11D7-8645000102C1865D

Klepeis, K.A. 1994. Relationship between uplift of the metamorphic core of the southernmost Andes and shortening in the Magallanes foreland fold and thrust belt, Tierra del Fuego, Chile. Tectonics 13 (4): 882-904. https://doi.org/10.1029/94TC00628

Klepeis, K.A.; Austin, J.A. Jr. 1997. Contrasting styles of superposed deformation in the southernmost Andes. Tectonics 16 (5): 755-776. https://doi.org/10.1029/97TC01611

Klepeis, K.A.; Betka, P.; Clarke, G.; Fanning, M.; Hervé, F.; Rojas, L.; Mpodozis, C.; Thomson, S. 2010. Continental underthrusting and obduction during the Cretaceous closure of the Rocas Verdes rift basin, Cordillera Darwin, Patagonian Andes. Tectonics 29 (3): TC3014. https://doi.org/10.1029/2009TC002610

Kohn, M.J.; Spear, F.S.; Dalziel, I.W.D. 1993. Metamorphic P-T Paths from Cordillera Darwin, a Core Complex in Tierra del Fuego, Chile. Journal of Petrology 34 (3): 519-542. https://doi.org/10.1093/petrology/34.3.519

Kohn, M.J.; Spear, F.S.; Harrison, T.M.; Dalziel, I.W.D. 1995. $^{40}Ar/^{39}Ar$ geochronology and P-T-t paths from the Cordillera Darwin metamorphic complex, Tierra del Fuego, Chile. Journal of Metamorphic Geology 13 (2): 251-270. https://doi.org/10.1111/j.1525-1314.1995.tb00217.x

Kranck, E.H. 1932. Geological investigations in the Cordillera of Tierra del Fuego. Acta Geographica Societas Geographica Fenniae 4: 1-231.

Lobo, C.; González Guillot, M.; Torres Carbonell, P.J.; Rodríguez, C.; Escayola, M.; Aragón, E.; Martín, G.; Garrido, C.J. 2024. Hallazgo de posible basamento de la cuenca Rocas Verdes en el sector Argentino de la Cordillera Fueguina. *In* Congreso Geológico Argentino, No. 22, Actas: 365-366. San Luis.

Maloney, K.T.; Clarke, G.L.; Klepeis, K.A.; Fanning, C.M.; Wang, W. 2011. Crustal growth during back-arc closure: Cretaceous exhumation history of Cordillera Darwin, southern Patagonia. Journal of Metamorphic

Geology 29 (6): 649-672. https://doi.org/10.1111/j.1525-1314.2011.00934.x

Martinioni, D.R.; Olivero, E.B.; Medina, F.A.; Palamarczuk, S.C. 2013. Cretaceous stratigraphy of Sierra de Beauvoir, Fuegian Andes (Argentina). Revista de la Asociación Geológica Argentina 70 (1): 70-95.

Mella, M.; Quiroz, D. 2023. Granito Svea: magmatismo Devónico-Carbonífero en Cordillera de Darwin, Tierra del Fuego, Chile. *In* Congreso Geológico Chileno, No. 16: 206 p. Santiago.

Mukasa, S.B.; Dalziel, I.W.D. 1996. Southernmost Andes and South Georgia Island, North Scotia Ridge: Zircon U-Pb and muscovite $^{40}Ar/^{39}Ar$ age constraints on tectonic evolution of Southwestern Gondwanaland. Journal of South American Earth Sciences 9 (5-6): 349-365. https://doi.org/10.1016/S0895-9811(96)00019-3

Nelson, E.P.; Dalziel, I.W.D.; Milnes, A.G. 1980. Structural geology of the Cordillera Darwin-Collisional-style orogenesis in the southernmost Chilean Andes. Eclogae Geologicae Helvetiae 73: 727-751.

Olivero, E.B.; Martinioni, D.R. 1996. Sedimentología de las Formaciones Lemaire y Yahgan (Jurásico-Cretácico) en Tierra del Fuego. *In* Congreso Geológico Argentino, No. 13 y Congreso de Exploración de Hidrocarburos, No. 3 , Actas 2: 45-59.

Olivero, E.B.; Martinioni, D.R. 2001. A review of the geology of the Argentinian Fuegian Andes. Journal of South American Earth Sciences 14 (2): 175-188. https://doi.org/10.1016/S0895-9811(01)00016-5

Olivero, E.B.; Medina, F.A.; López Cabrera, M.I. 2009. The stratigraphy of cretaceous mudstones in the eastern Fuegian Andes: new data from body and trace fossils. Revista de la Asociación Geológica Argentina 64: 60-69.

Olivero, E.B.; Torres Carbonell, P.J.; Bedoya Agudelo, E.L.; Gutiérrez, C.I.; Mosqueira González, V. 2025. Estratigrafía del Cretácico Superior-Cenozoico de las cuencas Austral-Malvinas en los Andes Fueguinos: actualización y síntesis. Revista de la Asociación Geológica Argentina 82 (1): 3-39.

Ortiz, M. 2007. Condiciones de formación del Complejo Metamórfico Cordillera Darwin, al sur de Seno Almirantazgo, Región de Magallanes, Chile. Memoria de título (Inédito), Universidad de Chile, Departamento de Geología: 114 p.

Palotti, P.; Menichetti, M.; Cerredo, M.E.; Tassone, A. 2012. A new U-Pb zircon age determination for the Lemaire Formation of Fuegian Andes, Tierra del Fuego, Argentina. Rendiconti Online Della Società Geologica Italiana 22: 170-173.

Passchier, C.W.; Trouw, R.A.J. 2005. Microtectonics. Springer: 366 p. Berlin.

Quensel, P. 1910. Geologisch-petrographische Studien in der patagonischen Cordillera. Bulletin of the Geological Institution of the University of Upsala 11: 1-114

Ramos, V.A. 2008. Patagonia: A paleozoic continent adrift? Journal of South American Earth Sciences 26 (3): 235-251. https://doi.org/10.1016/j.jsames.2008.06.002

Riley, T.R.; Burton-Johnson, A.; Flowerdew, M.J.; Poblete, F.; Castillo, P.; Hervé, F.; Leat, P.T.; Millar, I.L.; Bastías, J.; Whitehouse, M.J. 2023. Palaeozoic-Early Mesozoic geological history of the Antarctic Peninsula and correlations with Patagonia: Kinematic reconstructions of the proto-Pacific margin of Gondwana. Earth-Science Reviews 236: 104265. https://doi.org/10.1016/j.earscirev.2022.104265

Rojas, L.; Mpodozis, C. 2006. Geología estructural de la faja plegada y corrida de Tierra del Fuego, Andes Patagónicos Chilenos. *In* Congreso Geológico Chileno, No. 11: 325-328. Antofagasta.

Rossignol, C.; Hallot, E.; Bourquin, S.; Poujol, M.; Jolivet, M.; Pellenard, P.; Ducassou, C.; Nalpas, T.; Heilbronn, G.; Yu, J.; Dabard, M.-P. 2019. Using volcaniclastic rocks to constrain sedimentation ages: To what extent are volcanism and sedimentation synchronous? Sedimentary Geology 381: 46-64. https://doi.org/10.1016/j.sedgeo.2018.12.010

Sernageomin. 2003. Mapa Geológico de Chile. Servicio Nacional de Geología y Minería. Santiago. 1:1.000.000.

Sharman, G.R.; Malkowski, M.A. 2020. Needles in a haystack: Detrital zircon U-Pb ages and the maximum depositional age of modern global sediment. Earth-Science Reviews 203: 103109. https://doi.org/10.1016/j.earscirev.2020.103109

Söllner, F.; Miller, H.; Hervé, M. 2000. An Early Cambrian granodiorite age from the pre-Andean basement of Tierra del Fuego (Chile): the missing link between South America and Antarctica? Journal of South American Earth Sciences 13 (3): 163-177.

Suárez, M.; Pettigrew, T.H. 1976. An Upper Mesozoic island-arc-back-arc system in the southern Andes and South Georgia. Geological Magazine 113 (4): 305-328. https://doi.org/10.1017/S0016756800047592

Thomas, C.R. 1949. Manantiales field, Magallanes Province, Chile. AAPG Bulletin 33 (9): 1579-1589. https://doi.org/10.1306/3D933DF1-16B1-11D7-8645000102C1865D

Torres Carbonell, P.J.; Cao, S.J.; Dimieri, L.V. 2017. Spatial and temporal characterization of progressive deformation during orogenic growth: Example from the Fuegian Andes, southern Argentina. Journal of Structural Geology 99: 1-19. https://doi.org/10.1016/j.jsg.2017.04.003

Torres Carbonell, P.J.; Cao, S.J.; González Guillot, M.; Mosqueira González, V.; Dimieri, L.V.; Duval, F.; Scaillet, S. 2020. The Fuegian thrust-fold belt: From arc-continent collision to thrust-related deformation in the southernmost Andes. Journal of South American Earth Sciences 102: 102678. https://doi.org/10.1016/j.jsames.2020.102678

Twiss, R.; Moores, E. 2007. Structural Geology, 2nd edition. W.H. Freeman and Co.: 736 p. New York.

Vermeesch, P. 2018. IsoplotR: A free and open toolbox for geochronology. Geoscience Frontiers 9 (5): 1479-1493. https://doi.org/10.1016/j.gsf.2018.04.001

Vermeesch, P. 2021a. On the treatment of discordant detrital zircon U-Pb data. Geochronology 3 (1): 247-257. https://doi.org/10.5194/gchron-3-247-2021

Vermeesch, P. 2021b. Maximum depositional age estimation revisited. Geoscience Frontiers 12 (2): 843-850. https://doi.org/10.1016/j.gsf.2020.08.008

Wilson, T.J. 1991. Transition from back-arc to foreland basin development in the southernmost Andes: Stratigraphic record from the Ultima Esperanza District, Chile. Geological Society of America, Bulletin 103 (1): 98-111. https://doi.org/10.1130/0016-7606(1991)103%3C0098:TFBATF%3E2.3.CO;2

Manuscript received: September 29, 2025; revised/accepted: May 06, 2026; available online: May 11, 2026.